Universidade de Aveiro Departamento de Biologia
Ano 2013

Corine Santos Reis

Efeitos genotóxicos de nanopartículas de prata em células de pulmão

Genotoxic effects of silver nanoparticles on lung cells

DECLARAÇÃO

Declaro que este relatório é integralmente da minha autoria, estando devidamente referenciadas as fontes e obras consultadas, bem como identificadas de modo claro as citações dessas obras. Não contém, por isso, qualquer tipo de plágio quer de textos publicados, qualquer que seja o meio dessa publicação, incluindo meios eletrónicos, quer de trabalhos académicos.

Universidade de Aveiro Departamento de Biologia
Ano 2013

Corine Santos Reis

Efeitos genotóxicos de nanopartículas de prata em células de pulmão

Genotoxic effects of silver nanoparticles on lung cells

Dissertação apresentada à Universidade de Aveiro para cumprimento dos requisitos necessários à obtenção do grau de Mestre em Biologia Aplicada, realizada sob a orientação científica da Doutora Helena Cristina Correia de Oliveira, Investigadora de Pós-Doutoramento do Departamento de Biologia da Universidade de Aveiro e sob co-orientação científica da Professora Doutora Conceição Santos, Professora Associada com Agregação do Departamento de Biologia da Universidade de Aveiro e do Professor Doutor António Nogueira, Professor Associado com Agregação do Departamento de Biologia da Universidade de Aveiro.

Investigação realizada no âmbito do projecto "ASSAY - Avaliação do destino e efeitos de nanopartículas de prata em ecossistemas Aquáticos" financiado através do Programa Operacional Factores de Competitividade (COMPETE) com o n.º FCOMP-01-0124-FEDER-013952 (Refª. FCT PTDC/AAC-AMB/113649/2009).

Apoio financeiro do POCTI no âmbito do III Quadro Comunitário de Apoio.

Apoio financeiro da FCT e do FSE no âmbito do III Quadro Comunitário de Apoio.

Dedico este trabalho aos meus pais e irmã, por todo o apoio incondicional e por terem tornado possível esta óptima experiência.

o júri

Presidente	Prof. Doutor João António de Almeida Serôdio Professor Auxiliar do Departamento de Biologia da Universidade de Aveiro
Arguente principal	Prof. Doutora Isabel O' Neill de Mascarenhas Gaivão Professora Auxiliar na Universidade de Trás-os-Montes e Alto Douro, Centro de Ciência Animal e Veterinária
Vogal	Doutora Sónia Marina Pinto Nunes da Silva Investigadora Pós-Doutoramento no Departamento de Biologia da Universidade de Aveiro
Vogal	Doutora Ana Catarina Almeida Sousa Investigadora Pós-Doutoramento no CICS-UBI - Centro de Investigação em Ciências da Saúde, Universidade da Beira Interior
Orientadora	Doutora Helena Cristina Correia de Oliveira Investigadora Pós-Doutoramento, no Departamento de Biologia da Universidade de Aveiro

agradecimentos

A realização desta dissertação marca o fim de um percurso, com altos e baixos, mas quem em muito me realizou. Ao longo deste, várias foram as pessoas que contribuíram, de diferentes maneiras, para a sua concretização, às quais gostaria de expressar o mais sincero agradecimento.

Em primeiro, à Universidade de Aveiro e aos meus orientadores, sem os quais nada teria sido possível. À professora Conceição Santos por me ter aberto as portas do laboratório que dirige, e por todas as trocas de ideias. À Dra. Helena Oliveira, por todos os momentos de discussão, por me ter feito crescer muito enquanto bióloga. Ao professor António Nogueira, por todo o tempo que disponibilizou, por vezes fora de horário de trabalho, por toda a ajuda no tratamento estatístico dos dados, por me incentivar a superar os meus objectivos.

Um muito obrigado à Fê, por todo o tempo que disponibilizou para me passar os conhecimentos por ela adquiridos, por me ouvir, pelas discussões que proporcionou, e acima de tudo, pelos bons momentos de distracção, pela amizade que ficou. Aos meus colegas de laboratório, pelos conhecimentos que me proporcionaram, pelas boas discussões quando pensava que estava tudo perdido, por toda a ajuda.

À Inês, Noémia e Sara, por tudo. Pela amizade, pelos momentos de pura idiotice, por me ouvirem desabafar, pelo apoio que me deram nos momentos mais difíceis, por estarem sempre lá, para tudo.

À Sandra, que apesar da distância sempre me acompanhou. Por toda a amizade nestes últimos 5 anos, por ter aturado os meus dias menos bons, por ser a boa amiga que é.

À Bete, pelo apoio mutuo na escrita da dissertação, e pela óptima companheira de casa que se revelou.

Ao meu namorado, um especial obrigado. Por aturar o meu mau feitio, por me estender sempre a mão, pelo carinho, amor, sinceridade e positivismo que tanto precisei ao longo deste percurso.

Por último, mas em nada menos importante, um muito obrigado aos meus pais e à minha irmã, por todo o apoio, todo o amor, toda a paciência, por me ouvirem, por todos os bons conselhos que me deram, por terem tornado possível concluir uma etapa muito importante para mim.

A todos, o meu sincero e profundo obrigado.

palavras-chave

Nanopartículas de prata; A549; MG-63; genotoxicidade; ensaio de cometas; teste de micronúcleos por bloqueio de citocinese; efeito citostático; dano no DNA

resumo

As nanopartículas de prata têm grande importância pelas suas propriedades antimicrobianas sendo cada vez mais usadas, por exemplo, no revestimento de próteses, em material médico, no revestimento de embalagens alimentares e em cosmética. A sua crescente manufacturação reflectir-se-á também na sua existência no meio ambiente, como por exemplo, no ar, expondo o organismo aos seus potenciais efeitos prejudiciais. Este trabalho teve como objectivo a avaliação dos possíveis efeitos genotóxicos de nanopartículas de prata revestidas com polivinilpirrolidona. Para isso, usou-se uma linha celular de epitélio pulmonar, A549, que foi exposta a concentrações crescentes de 0, 50 e 100 µg/mL de nanopartículas de prata revestidas com PVP, de 10 e 20 nm, durante 24h. O teste dos micronúcleos por bloqueio da citocinese e o ensaio de cometas foram usados para avaliar os potenciais efeitos genotóxicos das nanopartículas de prata. Para validação do teste dos micronúcleos por bloqueio da citocinese, uma linha celular de osso, MG-63, foi exposta a concentrações crescentes de nanopartículas de prata revestidas com PVP, de 20 nm. Na linha celular A549, o ensaio de cometas revelou um aumento do dano no DNA com o aumento da concentração de nanopartículas de 10 nm. Por outro lado, os resultados obtidos para as nanoparticulas de 20 nm mostraram um aumento significativo da degradação do DNA apenas para a concentração mais baixa (50 µg/mL). O teste dos micronúcleos mostrou um efeito citostático das nanopartículas de prata. Na linha celular MG-63 verificou-se um aumento de micronúcleos e protusões nucleares para a concentração de 50 ug/mL, indicando a presença de dano no DNA. Em conjunto, os resultados sugerem que as nanopartículas de prata revestidas com PVP têm potencial para provocar dano no DNA, dependente da sua concentração e do seu tamanho, e têm um efeito citostático nas células.

keywords

AgNP; A549; MG-63; genotoxicity; comet assay; cytokinesis-block micronucleus cytome assay; cytostatic effect; DNA damage

abstract

Silver nanoparticles have increased importance due to their antimicrobial activity, being used in several applications such as in prosthesis, medical devices, food storing and cosmetics. Its increasing manufacturing will reflect in the environment, as for instance in the air, exposing the organism to its potential harmful effects. Altogether, the aim of this work was to evaluate the potential genotoxic effects of polyvinylpyrrolidone coated AgNPs. For that, a human alveolar adenocarcinoma cell line, A549, was exposed to increased concentrations of 0, 50 and 100 μg/mL PVP coated silver nanoparticles, of 10 and 20 nm, for 24h. Both the cytokinesis-block micronucleus cytome assay and the comet assay were used to evaluate the potential genotoxic effects of silver nanoparticles. To validate the cytokinesis-block micronucleus cytome assay, a human bone cell line, MG-63, was exposed to increased concentrations of 20 nm PVP coated silver nanoparticles. In A549 cell line, the comet assay revealed an increase in DNA damage, with increase concentration of silver nanoparticles of 10 nm. By other hand, for 20 nm AgNPs a significant increase in DNA damage was observed only for the lowest concentration (50 μg/mL). The cytokinesis-block micronucleus cytome assay showed a cytostatic effect of silver nanoparticles. In MG-63 cell line it was observed an increase in both micronucleus and nuclear buds for 50 μg/mL, indicating the presence of DNA damage. Altogether, the results suggest that PVP coated silver nanoparticles have the potential to induce DNA damage, dependent on the concentration and the size, and have a cytostatic effect on cells.

Index

List of Acronyms and Abbreviations

CBMN cyt assay	Cytokinesis-block micronucleus cytome assay
Cyt-B	Cytochalasin-B
EPA	Environmental Protection Agency
F-12K	Kaighn's Modification of Ham's F-12 Medium
FBS	Fetal Bovine Serum
GSH	Glutathione
LMP	Low Melting Point
MNi	Micronuclei
NBUDs	Nuclear Buds
NDI	Nuclear Diving Index
NMP	Normal Melting Point
NPBs	Nucleoplasmic Bridges
PBS	Phosphate Buffer Saline
POEM	Poly(oxyethylene)-segmented imide
PVA	Poly(vinyl alcohol)
PVP	Polyvinylpyrrolidone
ROS	Reactive Oxygen Species
SMA	Poly(styrene-co-maleic anhydride)-grafting poly(oxyalkylene)
SOD	Superoxide Dismutase

List of Figures

List of Tables

1.Introduction

1. Introduction

1.1. Historical overview

Nanotechnology study and works at the atom and molecular stage, and is considered, by the US Government's National Nanotechnology Initiative, "the understanding and control of matter at dimensions of roughly 1 to 100 nanometers, where unique phenomena enable novel applications." Its applications can across several science fields, such as engineering, materials science, physics, chemistry and biology (please see: http://www.nano.gov/ and http://www.nanotechproject.org/topics/nano101/introduction_to_nanotechnology/).

Although it is considered a modern science, there are records dating the 9th century of the use of nanomaterials (use of alternate-sized gold and silver particles by artisans of Mesopotamia to generate a sparkling effect to pots) [1]. By the year of 1857, Michael Faraday in "Experimental relations of gold (and other metals) to light" presented the first scientific description of the properties of nanoparticles [2]. In 1959, at an American Physical Society meeting at the California Institute of Technology, Richard Feynman gave the first talk about ideas and concepts behind nanoscience, entitled "There's plenty of space at the bottom". Only in 1974, however, the term nanotechnology was coined, by Professor Noro Taniguchi (please see http://www.nanotechproject.org/topics/nano101/introduction_to_nanotechnology/). Meanwhile, in the 1950's and 1960's, was held an enormous progress in the field of drug delivery by nanoparticles. One of the pioneers in this progress was Professor Peter Paul Speiser, which developed the first nanoparticle for drug delivery purpose and for vaccines [3]. In the early 1980's, with the development of new microscopes, the modern nanotechnology began, and in 1981 was published the first paper about it by K. Eric Drexler entitled "An approach to the development of general capabilities for molecular manipulation" [1]. With all the development made thenceforth, in the early 2000's start to appear the first consumer products that make use of nanotechnology in the market place (please see http://www.nanotechproject.org/topics/nano101/introduction_to_nanotechnology/).

Working at the nanoscale makes possible to scientists to use the unique physical, chemical, magnetic, optical and electric properties of nanomaterials, using them in a variety of applications such in sunscreens, in therapeutics as antimicrobian, in electronic devices and others. It is estimated, by the Lux Research, that by 2014 $2.6 trillion manufactured products will incorporate nanotechnology (please see http://www.nano.gov/).

Due to the special characteristics of nanomaterials, concern has arisen about the impact in human health and environment, becoming important to carry out studies about their toxicity [4,5].

1.2. Nanoparticles characterization and occurrence

Nanoparticles, (where the prefix “nano” is derived from the Greek “nanos” meaning “dwarf”) are particles with dimensions between 1-100 nm in one or more dimensions [6,7] . Due to its nano size, these particles have several unique properties, compared with their bulk materials, including large surface area per unit mass (which combined with the nano sized, increase their potential to cross cell membranes), high chemical reactivity (because of the larger surface area, the chemical reactivity is enhanced about 1000-fold) and high internal pore volumes [6,8].

Nanoparticles can occur due to natural processes (like photochemical reactions, volcanic eruptions, forest fires, erosion and by plants and animals) and anthropogenic sources (like engineered nanomaterials, and from by-products of combustion, food cooking, chemical manufacturing, combustion in vehicle and airplane engines and others) [6,8,9]. Also, due to the increasing use of nanomaterials, in the future one possible source of nanoparticles would be by the co-products of incinerated nanomaterials [10].

1.3. Classification

There are several aspects of nanoparticles that are important in their toxicity, like dimensionality, morphology, composition, uniformity and agglomeration, which are used to classify them. Regarding to the number of dimensions, they can be classified in one dimensional (1D), two dimensional (2D) or three dimensional (3D) nanoparticles (Fig.1A) [6]. Morphologically, nanoparticles can be divided in high- and low-aspect ratio (having in

account flatness, sphericity and aspect ratio) (Fig.1B) [6]. Based on composition, nanoparticles can be composed of a single material or be a composite of several materials (Fig.1C), the first ones synthesized and the second ones more present in nature [6]. Relatively to uniformity and agglomeration, and having in account the chemistry and the electro-magnetic properties of nanoparticles, they can exist as dispersed aerosols, as suspensions/colloids or in an agglomerate state (Fig.1D) [6]. To prevent this agglomerate state, and like that maintain the characteristics of nanoparticles, sometimes they are stabilized with coatings [5].

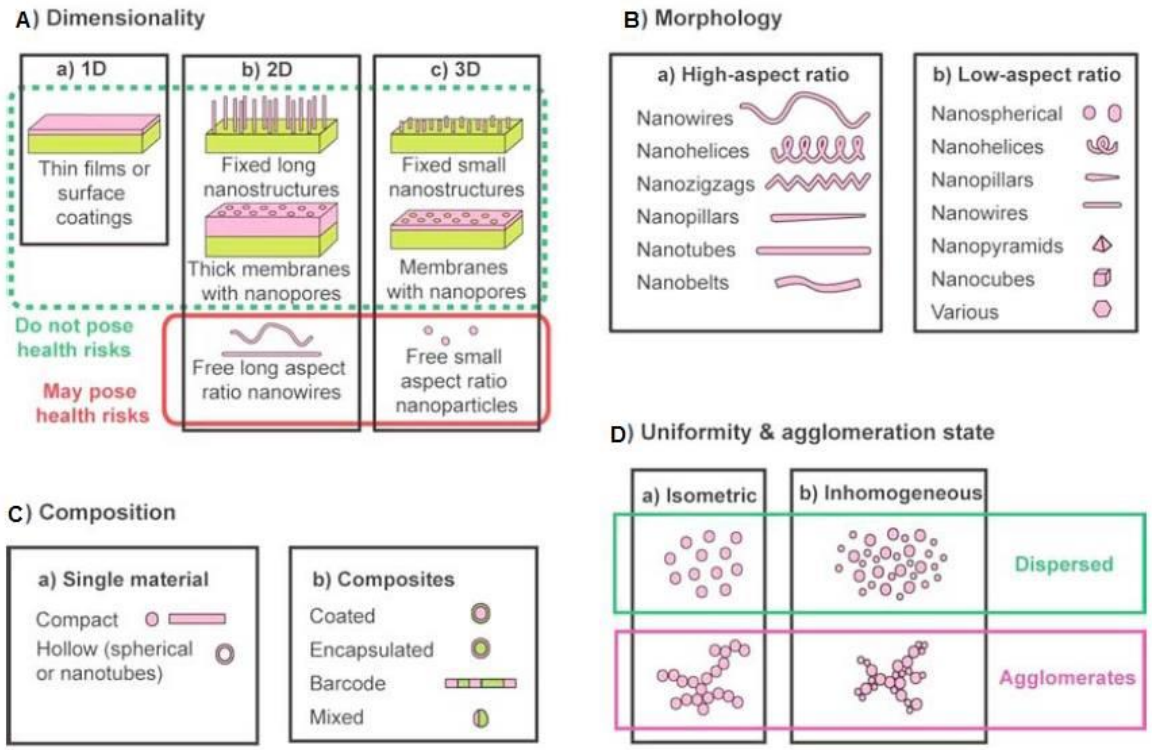

Fig. 1 Nanoparticles classification, having in account dimensionality (A), morphology (B), composition (C), uniformity and agglomeration state (D). Adapted from [6]

Despite the several existing classifications, according to EPA (please see http://www.epa.gov/fedfac/pdf/emerging_contaminants_nanomaterials.pdf) one can be:

- Carbon-based nanomaterials: composed mostly of carbon, with several electronic and biomedical applications. One example is the C60 fullerene;
- Metal-based materials: include quantum dots, nanogold, nanosilver and metal oxides (e.g. titanium dioxide). Have applications in drug release, remediation, as a UV blocker and in medical imaging;

- Dendrimers: nanosized polymers built from branched units, used for drug delivery, DNA transferring agents, among others;
- Composites: combination of two nanoparticles or nanoparticle with larger bulk type materials (an example of a bio-inorganic composite is a titanium molecule with DNA strands attached). Have important applications in drug delivery, cancer detection and to enhance mechanical and flame retardant properties in auto parts and packaging materials.

1.3.1. Applications

Due to its special characteristics, nanoparticles have a number of applications that cross a wide range of fields, from engineering to medicine or environmental sciences. Nanoparticles can be used in electronics, in transportation and telecommunication (nanoparticles of carbon black), in imaging (single-walled carbon nanotubes used as probe tips for atomic-force microscopy imaging of antibodies), in medical applications (like drug delivery, diagnostics and medical devices), in pollution remediation (due to their enhanced chemical activity), in cosmetics (like titanium dioxide and zinc oxide), in coatings (to provide antimicrobial characteristics, for example), in materials such as paint, in mechanical engineering and in food products [1,5,6].

1.4. Nanotoxicology

With the enormous potential that nanoparticles have, and since they are present in almost everything of our daily life, concerns must be taken considering the statement that all technology comes with a price.

There are several organs in constant contact with both engineered and natural nanoparticles, as skin, lungs and the gastro-intestinal tract. These are the most probable points of entrance to the organisms. Once inside the organism, and due to their small size, they can entry the cells and interact with the organelles [6]. This interaction may be beneficial, but may also be deleterious. Many studies have been done to understand the interaction between nanoparticles and cells, and several ones show a toxic effect to the organism. Li *et al.* [11] showed that lead sulfide nanoparticles (PbSNPs) induce oxidative damage in lung tissue. In the same tissue, Liu *et al.* [12] described that gold nanoparticles

(AuNPs) induce apoptosis and necrosis. Alarifis *et al.* showed that both copper oxide nanoparticles (CuONPs) [13] and zinc oxide nanoparticles (ZnONPs) [14] (in HaCat and A375 cell lines respectively), induce apoptosis and necrosis, and DNA damage mediated by oxidative stress. This type of DNA damage was also described by Ahamed *et al.* [15] in A431 and A549 cell lines induced by iron oxide nanoparticles (Fe_3O_4NPs).

Altogether, it is important to know and understand how nanoparticles interact with the organism, to better realize if the positive effects are greater than the negative ones.

1.5. Silver nanoparticles

Silver (Ag) is a shiny and white metallic element with number 47 in the periodic chart, with an atomic weight of 107.868 g mol^{-1}, a density of 10.49 g ml^{-1} and a valence of +1 or +2. With an occurrence of 0.1 ppm in earth's crust, it is a rare element known since ages, with applications in jewelry, utensils, monetary currency, dental alloy, photography, explosives etc. [16,17]. Ag compounds and ions have an important antimicrobial effect, used for both hygienic and healing purposes (dental work, catheters and burn wound for example) [16,18]. With the arise of manufactured silver nanomaterials, novel applications emerged, since they are considered to be more active due to their large surface area to volume ratio [19,20].

Silver nanoparticles (AgNPs), like other types of nanoparticles, are mostly smaller than 100 nm and contain 20-15,000 silver atoms [19]. Among the commercialized nanomaterials, AgNPs are the most used nanocompounds, predicted to be incorporated in approximately 25% of the products [21]. This huge interest in AgNPs is due to be an attractive material, that can be used in several fields for catalytic, optoelectronic, sensing and biotechnological applications [22]. Due to their unique antibacterial, antiviral and antifungal properties, AgNPs are being used in several clinical applications such as in surgery, in wound therapy and as an anti-inflammatory, and also in consumer products like in food storage materials, refrigerator surfaces, disinfectants, deodorants, in water purification, in toothpaste, shampoo, industrial products, kitchen utensils, toys, textiles and humidifiers [19,23–25]. Beyond that, AgNPs are used as a drug delivery vehicle, as biosensor, as an imaging contracts agent [26,27] and in the treatment of diseases that require targeting of specific cells or organs [26]. For instance, AgNPs have been shown to

interact with several viruses like HIV-1 [28] hepatitis B [29], respiratory syncytial virus [29], herpes simplex virus type 1 [30] and monkey pox virus [31].

With the range of applications of AgNPs there is high probability of getting exposed intentionally or not, to them. Therefore, information about their toxicity to biological systems, as is still not fully understood, should be a major concern.

1.5.1. Toxicity of AgNPs

In recent years several studies have emerged that establish new insights about AgNPs toxicity. Due to their small size, once they enter into the systemic circulation, they can easily migrate to other organs and tissues, like liver, spleen, lungs, kidneys and brain, where they can induce toxicity [22].The mechanism of uptake of AgNPs is still not clear, and several factors can influence it, like the morphology of nanoparticle, size, concentration, surface properties and the type of cell (different cells may have different mechanisms of uptake) [32]. Several studies found that the uptake usually happens by lipid raft-dependent endocytosis (caveolin-dependent), phagocytosis, clathrin-dependent endocytosis and macropinocytosis, the last two ones the most frequent [22,33,34].

Once inside the cell, the mechanism of toxicity may involve depletion of glutathione (GSH), increase of reactive oxygen species (ROS), reduction of the superoxide dismutase (SOD) enzyme activity and increase in lipid peroxidation [35–37]. All these factors lead to oxidative stress in the cell, which in mitochondria can lead to disruption of the mitochondrial respiratory chain and interruption of ATP synthesis. The oxidative stress can also lead to induction of DNA damage and finally to induction of apoptosis or necrosis [38,39]. AgNPs are also related with disturbances in cell cycle progression and induction of changes in gene expression, especially in the oxidative stress related genes [40,41].

As the mechanism of nanoparticle uptake, the outcome toxicity can be influenced by several factors like the size, the capability of agglomeration, the synthesis method and the surface chemistry of AgNPs, as well as the type of cell line. Regarding the nanoparticle size, studies showed that the smaller the nanoparticle, the higher the toxicity. That was verified in several cell lines, like in CaCo-2, where peptide-coated AgNPs of 20 nm induce more toxicity than the ones of 40 nm [42], and in cell lines 291.03C and RAW 264.7, where only the smaller nanoparticles were able to induce ROS [43]. In DC2.4, 3 nm

nanoparticles were able to induce toxicity at a concentration as low as 1 μg/mL [44]. However, it must be take into consideration, that different surface chemistries may also influence toxicity. Lin *et al*. [45] showed, that in HepG2 cell line, AgNPs stabilized with Poly(styrene-co-maleic anhydride)-grafting poly(oxyalkylene) (SMA) were less cytotoxic (despite being the smaller ones) than the ones stabilized with Poly(oxyethylene)-segmented imide (POEM) and Poly(vinyl alcohol) (PVA). Also, Sur *et al*. [21] showed that in HDF cell line, citrate reduced AgNPs (C-AgNPs) were more toxic than the modified ones with lactose (L-AgNPs) or a 12-base long oligonucleotide (O-AgNPs), and Kaur *et al*. [46] that AgNPs reduced with tannic acid (TSNPs) were more toxic than the ones reduced with sodium borohydride (BSNPs) (with the same sizes) in A431 and RAW 264.7 cell lines.

Beyond the importance of the nanoparticles characteristics, the cell line specificity is also important to consider, since the level of sensitivity may vary between cell lines. Studies realized with starch-coated AgNPs (6-20 nm) in IMR-90 and U251 cell lines, showed that the toxicity was more prominent in U251 [38]. In RAW 264.7, A498, HepG2 and Neuro2A cell lines, the toxicity was evaluated for 40 nm AgNPs, and it was observed that the cell lines A498 and RAW 264.7 were more sensitive, showing toxic effects already for 1 or 3 μg/mL, respectively [22].

In many studies, isolated AgNPs or aggregations inside the cell were observed, specifically in the cytoplasm, inside lysosomes, nucleus and inside mitochondria [22,47]. The uptake of AgNPs inside the nucleus is of huge interest, because once there, they can interact directly with the DNA, and induce damage (in addition to the induced by the generation of oxidative stress). In fact, consequences like G2/M arrest, S-phase arrest and DNA damage was described in several studies [38,47–49].

Beyond the AgNPs, the silver ions (Ag^+ ions) released from them also play an important role in the toxicity mechanism, being considered, by some authors, more toxic than the AgNPs themselves [38]. Beer *et al*. [50] described that the toxicity of AgNP suspension depends strongly in the initial amount of silver ions, in A549 cells, whereas Kim *et al.* [51] described that AgNPs exhibited cytotoxicity with the same potency that silver ions in HepG2 cells. These controversies results justify the importance of evaluate the amount of silver ions within the investigated AgNP suspensions.

Looking at recent studies done in A549 cell line, almost all the sizes of AgNPs used are large (above 30 nm), and almost all concerned in the cytotoxicity evaluation. This study concerns, thereby, in the evaluation of the genotoxic effects of smaller nanoparticles, of 10 and 20 nm.

1.6. Genotoxicity assessment

The genomic DNA is constantly under threat, and sometimes suffers damage that can be caused by factors as exposure to chemicals, nutrition or cellular processes such as action of endogenous ROS and stochastic errors in replication or recombination [52,53]. The alterations in the genetic material (genotoxicity) are one of the examples of cellular toxicity, and since they are highly correlated with an increased risk of cancer, is very important that they are assessed [4]. Two important tests used to determine genotoxicity are the comet assay and the cytokinesis-block micronucleus cytome assay [4,54].

1.6.1. Comet assay

The comet assay, or single-cell gel electrophoresis, was first described and developed by Östling and Johanson in 1984 [55], with the migration of DNA from single cells in a microgel. In 1988, Singh et al. [56] developed the current and most commonly used variation: the alkaline comet assay.

The comet assay combines the simplicity of biochemical techniques for detecting DNA single strand breaks, alkali labile sites and cross-linking, with the single cell approach typical of cytogenetic assays [57,58]. It is based on the ability of negatively charged loops/fragments of DNA to migrate out of the cell in the direction of the anode, under electrophoretic conditions [57,59]. When viewed under a microscope, the cells get the appearance of a ‘comet’, with a head (nuclear region) and a tail containing DNA fragments (Fig.2).

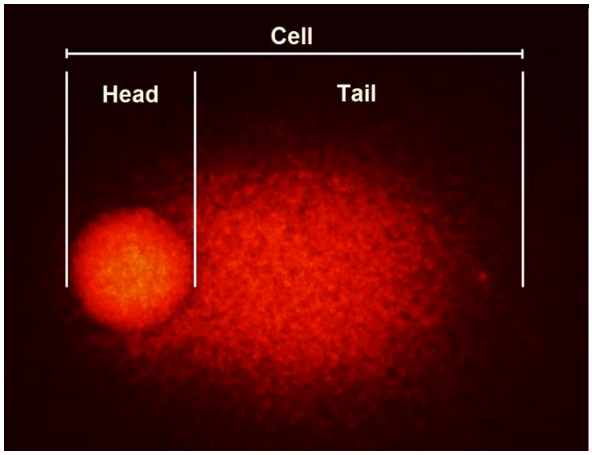

Fig. 2 Illustrative image of a cell after the performance of the comet assay, viewed under a microscope, showing its typical appearance.

The size and the shape of the comet, and the distribution of the DNA within the comet, correlate with the extent of DNA damage [59]. The damage is posteriorly assessed by visual scoring (based on the tail length and the shape, the comets are classified qualitatively in five categories) or using a software of image analysis, that recognizes the extension of the damage. When using the software analysis, several parameters are measured, being the most relevant the % tail DNA, tail length and tail moment [57].

The comet assay has been widely used in research by investigators, and compared with other genotoxicity assays has several advantages as: (1) analyses at the level of the individual cell, (2) requirement for small number of cells per sample, (3) sensitivity for detecting low levels of DNA damage, (4) use of any eukaryote single cell population, (5) flexibility, (6) low costs, (7) easiness and quickness [60,61], and the detection of many kinds of damage by the use of repair enzimes [62]

1.6.2. Cytokinesis-block micronucleus cytome assay

The cytokinesis-block micronucleus cytome assay (CBMN cyt assay) is recommended as an in vitro genotoxicity testing method to characterize the genotoxicity of nanoparticles [63,64]. This test allows the measurement of DNA damage, cytostasis and cytotoxicity (Fig.3) [65]. In the CBMN cyt assay, the cytokinesis is blocked in cells that have completed one nuclear division by the addition of cytochalasin-B (Cyt-B). Cyt-B is an inhibitor of actin polymerization of the microfilament ring, required for the completion of

cytokinesis. By that, its use enables the accumulation of once-divided cells, recognized by their BN appearance [64,65].

DNA damage is measured in once-divided binucleated (BN) cells by scoring of micronuclei (MNi), nucleoplasmic bridges (NPBs) and nuclear buds (NBUDs). MNi are expressed in dividing cells, and can be originated by acentric fragments (chromosome fragments lacking a centromere) or whole chromosomes that are unable to migrate to the spindle poles during anaphase [66]. NPBs are biomarkers of DNA misrepair and/or telomere end-fusions. They can occur between nuclei in binucleated cells and are probably dicentric chromosomes in which the two centromeres were pulled to opposite poles of the cell and the DNA in the resulting bridge is covered by nuclear membrane [65,66]. NBUDs are biomarkers of elimination of amplified DNA and/or DNA repair complexes. NBUDs are characterized by having the same morphology as an MN with the exception that they are linked to the nucleus by a narrow or wide stalk of nucleoplasmic material [65]. Cytostasis is measured via the proportion of mono-, bi-, and multinucleated cells and cytotoxicity via necrotic and/or apoptotic cell ratios [65].

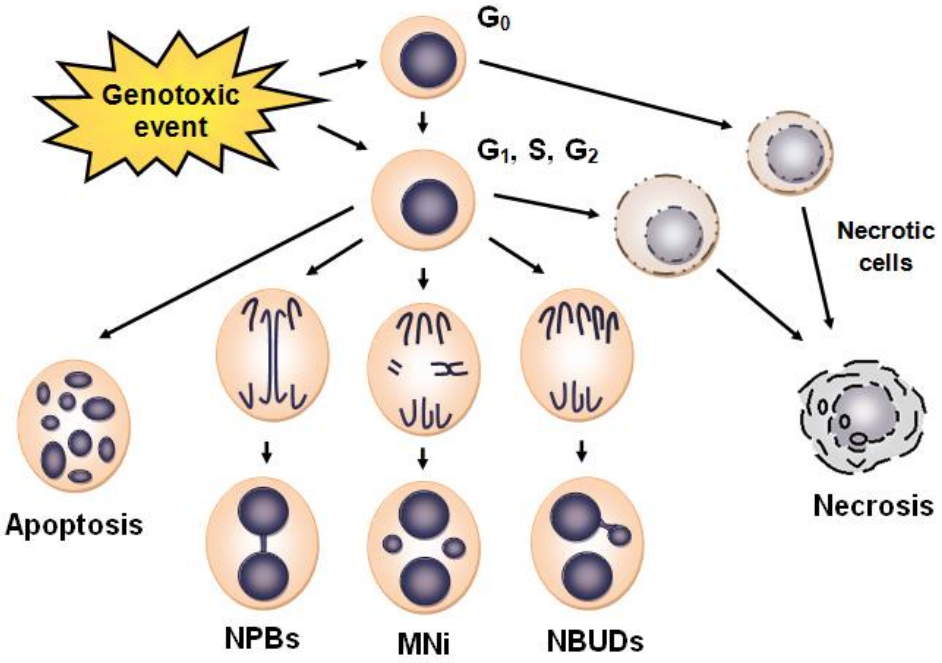

Fig. 3 Schematic figure of the cytokinesis-block micronucleus cytome assay (CBMN cyt assay), used to test the genotoxicity of nanoparticles. After the genotoxic event, the DNA damage is measured in once-divided binucleated cells by scoring NPBs, MNi and NBUDs. The test also allows the measurement of cytotoxicity via apoptotic and/or necrotic cell ratios. Adapted from Fenech [65]**.**

1.7. Cell line – A549

The lungs are organs extensively exposed to AgNPs, related to one possible route of exposure – inhalation [4,67], being important to understand its interaction with silver nanoparticles. For that, the in vitro cell model used in this study was A549 (human alveolar adenocarcinoma cell line).

A549 cell line was established in 1972 and is derived from human lung adenocarcinoma. These cells exhibit characteristic features of Type II cells of the pulmonary epithelium, such as growth as an adherent monolayer, presence of multilamellar cytoplasmic inclusions bodies and synthesis of lecithin with high percentage of disaturated fatty acids [68,69].

1.8. Aims

Although the wide usage of AgNPs with purposes of antimicrobial activity or drug delivery, studies concerning their genotoxicity are still scarce. This study aimed the evaluation of the genotoxic effects of polyvinylpyrrolidone (PVP) coated AgNPs of two different sizes (10 and 20 nm) in a human lung cell line – A549. The cell line was cultivated in vitro and exposed to increased concentrations of PVP coated AgNPs and genotoxicity was later assessed by the comet assay and the CBMN cyt assay.

2. Materials and Methods

2. Materials and methods

2.1. A549 Human alveolar adenocarcinoma cell line and MG-63 cell line cultures

The human cell line A549 was purchased from Sigma-Aldrich (St. Louis, MO, USA). A549 cell line was cultured in vitro in a controlled humid atmosphere of 5% CO_2 at 37°C, under aseptic conditions ensured by working on a laminar flow biological safety cabinet. Cells were cultured in 75 cm^2 culture flasks (Corning®), with 10 mL of complete growth medium. The complete growth medium was composed of Kaighn's Modification of Ham's F-12 Medium (F-12K), supplemented with 10% (v/v) Fetal Bovine Serum (FBS), 10000 units ml^{-1} of penicillin-streptomycin and 2.5 μg/ml of Fungizone, all purchased from Life Technologies (Carlsbad, CA, USA). Before cells reach approximately 80% confluence, (percentage of cell coverage on the surface area of the culture vessel), which happens approximately every three days, they were subcultured.

The culture conditions of MG-63 cell line were equivalent to the culture conditions of A549 cell line, with the exception of the complete growth medium: in A549 the complete growth medium was composed of Kaighn's Modification of Ham's F-12 Medium (F-12K) with the described supplementations, while in MG-63 was composed of α-MEM – Minimum Essential Medium (Gibco), with the same described supplementations,

2.2. Trypsinization

In order to subculture both A549 and MG-63 cells, a proteolytic enzyme (trypsin) was added, so that the cell-to-cell and cell-culture vessel adhesions can be digested. Before subculture, cells were observed under an inverted microscope to verify confluence, morphology and presence of contaminants. After removing culture medium, cells were washed with sterile phosphate buffer saline (PBS) at pH 7.2, purchased from Life Technologies (Carlsbad, CA, USA). Next, cells were incubated for 5 minutes at 37°C with 0.25% trypsin/1mM EDTA purchased from Life Technologies (Carlsbad, CA, USA), and complete detachment and dissociation was verified under microscope. At that time, complete growth medium was added (2x the trypsin volume added to cells) to inactivate trypsin action. After cell resuspension and determination of cell density (using a Neubauer chamber), complete growth medium and cell suspension (on a proportion of

1:9 – cell suspension: complete growth medium) were added to a new culture flask properly identified (with cell passage, cell type, username and date).

2.3. AgNP Exposure

The AgNPs used in this study were spherical, well defined sizes particles of 10 and 20 nm, coated with Polyvinylpyrrolidone (PVP) (BioPure - 1.0 mg/ml), obtained from NanoComposix (San Diego, CA, USA). In order to obtain the desired dilutions, the stock solution was diluted in complete growth medium (F12K) and sonicated for 20 minutes.
Cells were subcultured to multiwell plates and incubated for 24h in the normal culture conditions for adherence. After that time, the culture medium was replaced by the same amount of new growth medium with the desired final dilutions of AgNPs – 0, 50, 100 µg/mL, and cells were exposed for 24h. The final dilutions of AgNPs were chosen having in account the results of the cell viability test of a previous study done under the same conditions (Rosário, 2012, Effects of silver nanoparticles on osteosarcoma and lung cell lines, UA, Aveiro, Portugal).

2.4. DNA damage

2.4.1. Comet assay

The comet assay was performed as described by Singh et al. [56] and Tice et al. [70] with slight modifications. Slides with frosted ends were dipped into a solution of 1% normal melting point (NMP) agarose and the dried overnight at room temperature. After exposure ending, cells were harvested, counted in Neubauer chamber and then transferred to microtubes. Cells were then centrifuged at 700 g for 5 minutes at 4ºC. The supernatant was removed, the pellet dispersed in PBS and centrifuged again. After the last centrifugation, the supernatant was removed and the pellet was dispersed in PBS having into account that the cellular density should be such that each gel contains approximately $2x10^4$ cells. For positive control, cells were incubated with 100 µM H_2O_2 exactly for 10 minutes. For that, they were centrifuged for 5 minutes and right before the end of 10 minutes of the H_2O_2 treatment, they were resuspended in PBS. On each slide with the dried NPM agarose layer were spread two gels, consisting in a mixture of 50 µL of the cell suspension and 50 µL of 1% low melting point (LMP) agarose previously heated

at 37 ºC.A coverslip was placed over each mixture and the agarose was allowed to solidify at 4°C for at least 10 minutes. Cells were then lised in a solution containing 2.5 M NaCl, 100 mM Na_2EDTA, 10mM Trizma Base, 10 M NaHO, corrected pH 10, and 2% Triton X-100. Coverslips were removed and cells were then treated with lysis solution for 1h30. Meanwhile, electrophoresis buffer was freshly prepared with chilled distilled water and with 10 mM NaOH and 200 mM Na_2EDTA, pH 13. The reaction of lysis was stopped by placing slides on cold plate on ice and then the slides were immersed in an electrophoresis box with the cold electrophoretic buffer for 20 minutes (to allow DNA unwinding). Thereafter, electrophoresis ran for 30 minutes, 0.8 V/cm, 300 mA. Since lysing step until the end of electrophoresis, slides were kept in the dark avoiding direct fluorescent light to cause DNA damage. Next, slides were neutralized by rinsing in 1% PBS at 4°C, twice for 10 minutes. Slides were left overnight to dry. To perform comet scoring, the slides were rehydrated for 30 minutes with cold dH_20 and stained with 20 µg/mL ethidium bromide for 20 minutes, removing the excess with cold dH_20. Slides were observed under a fluorescence microscope Nikon Eclipse 80i equipped with an excitation filter of 510-560 nm and a barrier filter of 590 nm. For each treatment group, one slide (with two gels) from each well was screened and 50-100 randomly visualized nucleoids were picked. Images were captured with imaging software (NIS-Elements F 3.00, SP7). Each image was run on version 1.2.2 of CASPLab – Comet Assay Software Project to automatically score a comprehensive set of parameters such as % tail DNA, tail length and tail moment, to provide a global comet description.

2.4.2. Cytokinesis-block micronucleus cytome assay

The cytokinesis-block micronucleus cytome assay was performed as described by Fenech [65] with slight modifications. Cells were seeded in 6 well-plates, using one coverslip per well. After 24h of cell adhesion, cells were exposed to AgNPs and to 25 µg/mL of methyl methanosulfonate (MMS) as positive control. After exposure, cytochalasin B (4.5 µg/mL) was added to each well and let incubate for 29 h. Cells were then fixed with absolute methanol cooled at 4°C. The coverslips were collected from the wells, properly identified and stored. To analyze micronuclei, the coverslip was stained with 1% acridine orange and mounted with cold distilled water. Slides were observed

under a fluorescence microscope Nikon Eclipse 80i equipped with an excitation filter of 450-490 nm and a barrier filter of 520 nm. To obtain the nuclear division index, the number of viable cells with one, two, three or four nuclei were count in at least 500 cells per slide. The number of necrotic and apoptotic cells was also scored in 500 cells per slide. To detect and count MNi, NPBs and NBUDs a minimum of 1000 binucleated cells were scored per slide.

2.5. Statistical Analysis

All data are expressed as mean ± standard deviation (SD). The statistical analysis was performed using SigmaPlot for Windows version 11.0 (Systat Software Inc., San Jose, CA, USA).

The assessment of statistical significance between control and AgNP-treated groups was performed using one-way or two-way analysis of variance (ANOVA) followed by post-hoc testing (Tukey test) whenever significant differences were found. When the normality and homoscedasticity failed, a Kruskal-Wallis One Way Analysis of Variance on Ranks was performed (when comparing NP concentrations) or the Mann-Whitney Rank Sum test when only two groups were involved (i.e. when comparing NP sizes). All statistical tests used a level of significance of 0.05.

Comet data, prior to statistical analysis, was normalized relative to control. Thus, both tail length and tail DNA were transformed as

$$Tail_{relative} = \frac{Tail_{Ctrl} - Tail_{Treat}}{Tail_{Ctrl}},$$

where $Tail_{relative}$ represents the normalized variable (tail length or tail DNA), $Tail_{ctrl}$ is the average response in the control and $Tail_{treat}$ is the measured response in the treatment.

3. Results and Discussion

3. Results and discussion

3.1. Cell morphology and confluence

Cells were daily observed under an inverted microscope to check confluence, putative contaminations and morphology.

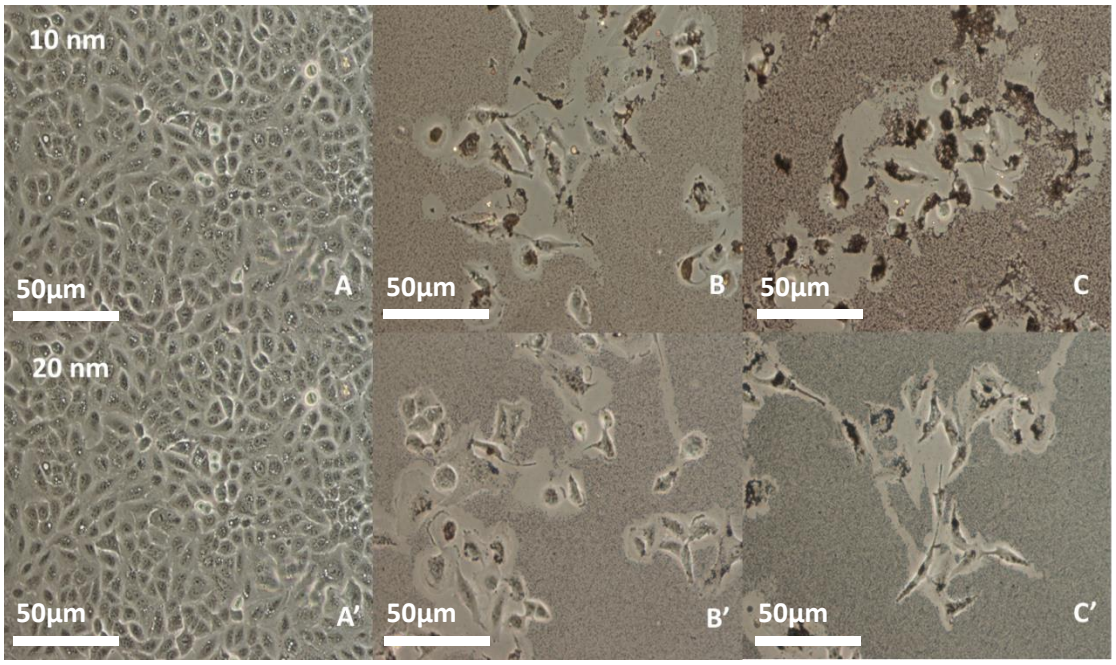

Fig. 4 Light microscopy images of A549 cells exposed to AgNPs for 24h: A, A' - control; B, B' -50 µg/mL; C, C' – 100 µg/mL.

After exposure of cells to AgNPs, for both sizes was noticed a decrease in confluence (number of cells) and a change in shape and morphology of cells. In control group, A549 cells presented a typical cuboidal epithelial aspect, which is indicative of type II pulmonary morphology, and colonized all the space available, after the 24h treatment (Fig.4A and A'). When exposed to AgNPs, cells appeared with an irregular aspect, most of them fusiform, and with less contacts with the neighbors. Similar results were also described by Lee *et al.* [71], also in A549 cells treated with AgNPs. Also, in AgNPs exposed cells the confluence was much lower comparatively to the control, realized by the space available in the end of the 24h treatment (Fig.4 B, B', C and C'). These observations are probably related with an unhealthy status of the cells and are markedly visible even for the lowest concentration (50 µg/mL). These results may suggest disturbances of cytoskeletal functions caused by AgNPs, already questioned by Asharani *et al.* [38]. Other

groups also described similar effects in other cell lines and nanoparticles, like described for A375 cell line treated with ZnONPs [14].

Dark clumps of AgNPs adsorbed on the cell surface were also seen, after treatment with AgNPs. For both 10 and 20 nm AgNPs, in the 50 μg/mL group, the results were equivalent, with some dark clumps existing (Fig.4B and B'). For the 100 μg/mL group, however, markedly differences could be observed when comparing 10 and 20 nm AgNPs. For 20 nm AgNPs, only a small difference exists in the dark clumps in 100 μg/mL compared to the lower concentration (Fig.4C'), but for 10 nm AgNPs was possible to see a markedly increase in the existing dark clumps (Fig.4C). This observations are somehow in agreement with a previous study done in the same conditions, where Rosário (Rosário, 2012, Effects of silver nanoparticles on osteosarcoma and lung cell lines, UA, Aveiro, Portugal) described, with the Dynamic Light Sacttering (DLS) test, that for 20 nm AgNPs the hydrodynamic diameter (nm) decreases from 93.93 (for 50 μg/mL) to 48.04 (for 100 μg/mL) and for 10 nm AgNPs the hydrodynamic diameter increases from 47.85 (for 50 μg/mL) to 84.05 (for 100 μg/mL). That can suggest that the AgNPs of 10 nm may have more tendency to aggregate than the ones of 20 nm, maybe due to fact that smaller nanoparticles have larger surface area being more reactive and, therefore, interacting more [6,72]. Other studies also states that the behavior of aggregation increase with the concentration of nanoparticles [73].

3.2. DNA damage

A direct consequence of DNA damage is chromosome abnormalities, like single strand breaks, alkali labile sites and cross-linking, that can be measured by two tests – the comet assay and the CBMN cyt assay.

3.2.1. Comet assay

The images obtained by fluorescence microscopy reflected the tendency of the parameters studied. For 10 nm AgNPs, it was possible to see a bigger tail as the concentration of AgNPs increased (from 0 to 100 μg/mL), reflecting an increase in the percentage of DNA on it (Fig.5).

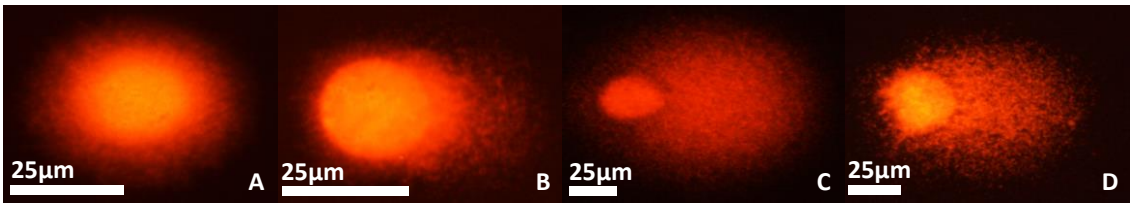

Fig. 5 Representative images obtained by fluorescence microscopy of the comet assay, for 10nm: A) control, B) 50 µg/mL, C) 100 µg/mL and D) positive control.

Analyzing the parameter 'Relative Tail length' (Fig.6A), a significant difference between AgNPs of 10 and 20 nm (Mann-Whitney Test, T = 208.000, n_1= 16, n_2= 17; P = 0.022) was observed, however the same was not seen for the parameter 'Relative Tail DNA' (Fig.6B) (Mann-Whitney Test, T = 297.000, n_1= 16, n_2= 16; P = 0.221).

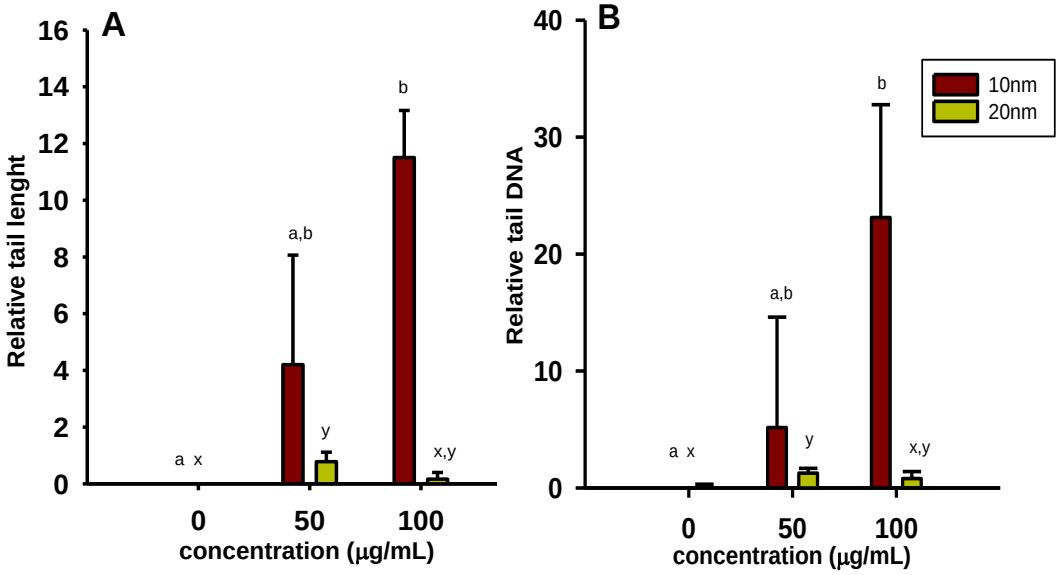

Fig. 6 DNA damage in A549 cell line exposed to 10 and 20 nm AgNPs using the comet assay and the parameters Relative tail length (A) and Relative tail DNA (B). Different letters means statistic differences between groups (p<0.05), where a and b refers to 10 nm AgNPs, and x and y to 20 nm AgNPs.

Looking at the 10 nm AgNPs (Fig.6A and B), was possible to see a concentration dependent increase in both parameters, with the 100 µg/mL group being significantly different from the control group ('Relative Tail Length': Kruskal-Wallis test, H = 12.923, df=2, P = 0.002; 'Relative Tail DNA': Kruskal-Wallis test, H = 12.458, df=2, P = 0.002). As the length of the comet tail increases with the extent of the DNA damage, after exposure to 10 nm AgNPs, it was, therefore, possible to observe an increase in DNA damage with increase nanoparticle concentration. The same tendency of a concentration dependent

increase in DNA damage was also previously described in literature. It was described that the cell lines U251 and IMR-90 have that tendency when treated with increased concentrations of AgNPs [38] and the same was described for A549 cell line when treated with other types of nanoparticles, like CeO_2NPs [74] and MFI nanoparticles [75].

For AgNPs of 20 nm (Fig.6A and B), the amount of DNA damage, evaluated with both parameters was significant only for the 50 µg/mL group ('Relative Tail Length': Kruskal-Wallis test, H = 10.283, df=2, P = 0.006; 'Relative Tail DNA': Kruskal-Wallis test, H = 11.765, df=2, P = 0.003). This result may be explained by the statement that higher sizes of nanoparticles, along with the behavior of agglomeration, may not be able to enter so easily in cells, as smaller ones [76]. A previous study done by Kruszewski *et al.* [77] also reported a slight decrease (although not significant) between the concentrations 50 and 100 µg/mL, when A549 cells where treated with 20 nm AgNPs.

Although the parameter "tail moment" is commonly used in many studies to evaluate the DNA damage [38,75,78], it has the disadvantage that there are no standard units (once it is the product of tail intensity x tail length), adding little information about the level of damage presented [79]. Therefore, it was decided not to include this parameter.

3.2.2. Cytokinesis-block micronucleus cytome assay

When performed the CBMN cyt assay, some images were taken, that represents well the tendency of the parameters studied (Fig.7)

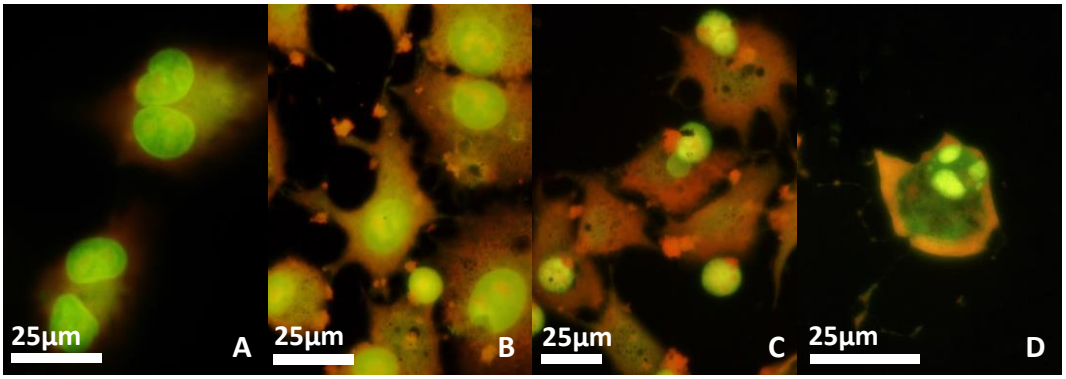

Fig. 7 Representative images obtained by fluorescence microscopy of the cytokinesis-block micronucleus cytome assay in A549 cells: A) binucleated cells (control), B) mononucleated cells (100 µg/mL 20 nm AgNPs), C) necrotic cells (50 µg/mL 20 nm AgNPs) and D) apoptotic cell (50 µg/mL 10 nm AgNPs).

After exposure to both 10 and 20 nm AgNPs, it was observed a marked decrease in the number of binucleated cells (Fig.7A and Fig.8), and therefore an increase in mononucleated ones (Fig.7B and Fig.8), for both concentrations, when compared to control (statistical analysis represented in table 1 and 2). Statistical analysis showed no differences between AgNPs sizes.

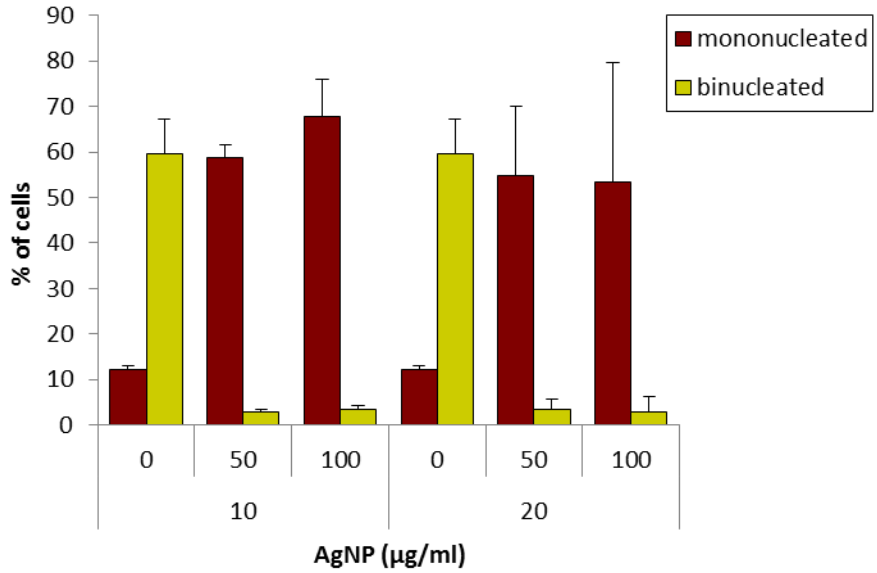

Fig. 8 Percentage of mono and binucleated cells assessed with the cytokinesis-block micronucleus cytome assay, after exposure of A549 cells to 10 and 20 nm AgNPs. Results are expressed as means ± standard deviation.

Table 1 Statistical analysis for Mononucleated cells: Two Way Analysis of Variance

	F	DF	P	Tukey-test
NP Concentration	25.923	2	<0.001	[0]≠[100]=[50]
NP Size	1.008	1	0.335	10nm=20nm
Interaction	0.513	2	0.611	

Table 2 Statistical analysis for Binucleated cells: Two Way Analysis of Variance

	F	DF	P	Tukey-test
NP Concentration	303.767	2	<0.001	[100]=[50]≠[0]
NP Size	0.000423	1	0.984	10nm=20nm
Interaction	0.0258	2	0.975	

When calculated the NDI, it was observed a markedly decrease when the cells were treated with both 50 and 100 μg/mL of AgNPs, with no differences between AgNPs of 10 and 20 nm (statistics represented in table 3). This observation also reflects the large number of mononucleated cells, once it is far from the ideal value of 2 [65], when all the cells are binucleated (Fig.9).

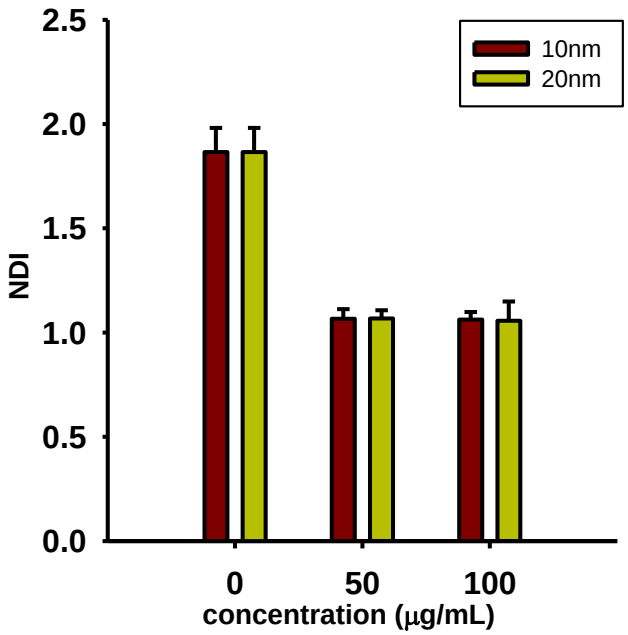

Fig. 9 Nuclear division index (NDI) assessed by the cytokinesis-block micronucleus cytome assay, after exposure of A549 cells to 10 and 20 nm AgNPs. Results are expressed as mean ± standard deviation

Table 3 Statistical analysis for the NDI: Two Way Analysis of Variance

	F	DF	P	Tukey-test
NP Concentration	1179.826	2	<0.001	[100]=[50]≠[0]
NP Size	0.00674	1	0.936	10nm=20nm
Interaction	0.0172	2	0.983	

When evaluated the number of necrotic and apoptotic cells, it was seen that the number of cells under death was high, even in the control group, predominantly in necrosis (statistics represented in table 4 and table 5), having no differences between cells treated with 10 or 20 nm AgNPs (Fig.10). In apoptosis, the significant differences

occurred only between 50 µg/mL and 100 µg/mL. In necrosis, the 50 µg/mL group was significantly different from the control and from 100 µg/mL.

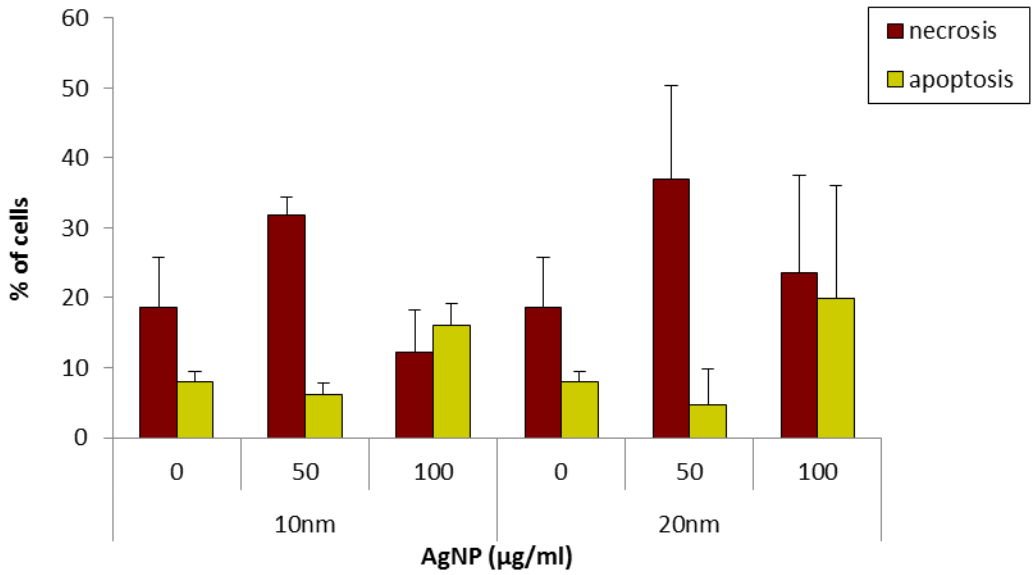

Fig. 10 Percentage of necrotic and apoptotic cells assessed with the cytokinesis-block micronucleus cytome assay, after exposure of A549 cells to increasing concentrations of 10 and 20 nm AgNPs. Results are expressed as means ± standard deviation.

Table 4 Statistical analysis for necrosis evaluation: Two Way Analysis of Variance

	F	DF	P	Tukey-test
NP Concentration	5.979	2	0.016	[100]=[0]≠[50]
NP Size	1.583	1	0.232	10nm=20nm
Interaction	0.561	2	0.585	

Table 5 Statistical analysis for apoptosis evaluation: Two Way Analysis of Variance

	F	DF	P	Tukey-test
NP Concentration	5.313	2	0.022	[50]≠[100]
NP Size	0.0482	1	0.830	10nm=20nm
Interaction	0.230	2	0.798	

Taken together the previous observations, the existence of more mononucleated cells than binucleated ones, and the markedly reduction of the NDI after treatment with AgNPs, may be explained by the cytostatic effect induced by AgNPs on cells, previously described by other authors [80]. In fact, it was described in a previous report by Rosário (Rosário, 2012, Effects of silver nanoparticles on osteosarcoma and lung cell lines, UA, Aveiro, Portugal), that both 10 and 20 nm AgNPs induced cell cycle arrest at G2/M phase in A549 cell line. Although is not consensual what type of arrest AgNPs may induced, it was described by other authors the same tendency of an arrest at G2/M phase [71,81]. The cell cycle arrest at G2/M phase was described previously by some authors, to be related with the progression of cells to apoptosis [82,83]. Rosário (Rosário, 2012, Effects of silver nanoparticles on osteosarcoma and lung cell lines, UA, Aveiro, Portugal) described also a decrease in the number of viable A549 cells and an increase in the number of late apoptotic ones, in accordance to the cell cycle analysis. This tendency was observed, however, only for 10 nm AgNPs. Also, almost none necrotic cells were observed, for both sizes of AgNPs. In the present study, the number of both apoptotic and necrotic cells was high even in the control group. One possible explanation for these high baseline levels, along with the large number of mononucleated could be due to the use of cyt-B *per se*, rather than due to the AgNPs. The large number of mononucleated cells may be explained by a not sufficient time of exposure to cyt-B, in order to cells recover its cycle, and the high number of cells in cellular death, mainly in necrosis, due to a possible over high concentration of cyto-B, toxic to cells.

According to Fenech [65], the scoring of the CBMN cyt assay related parameters MNi, NBUDs and NPBs should be performed in binucleated cells, meaning an ideal NDI value of 2. Since the NDI was near 1 for both concentrations of AgNPs tested, the requirements for measuring DNA damage were not totally accomplished in this study. In order to improve the test, the concentration of cyt-B and time of exposure were optimized. Some previous studies indicate that A549 cell line is more sensitive to lower concentrations of NP, when compared to other cell lines. De Marzi *et al.* [74] described that for 0.5 µg/mL of CeO_2NP, A549 cell line was the most sensitive, compared to CaCo2 and HepG2 cell lines. Furthermore, Rosário (Rosário, 2012, Effects of silver nanoparticles

on osteosarcoma and lung cell lines, UA, Aveiro, Portugal) compared the MG-63 and A549 cell lines, and found that A549 was more sensitive, once the results obtained for the cell cycle analysis for 50 µg/mL in A549 cell line were comparable with the ones obtained for 100 µg/mL in MG-63. Also, no significant apoptotic or necrotic cells were observed in MG-63 cell line, whereas in A549 was significant already for 24h of AgNP treatment (Rosário, 2012, Effects of silver nanoparticles on osteosarcoma and lung cell lines, UA, Aveiro, Portugal). Therefore, the osteoblast like cell line MG-63 was chosen as a less sensitive cell line to be a model for the optimization of the CBMN cyt assay conditions, specifically in what concerns to Cyt-B concentration and duration of the incubation. The MG-63 cell line is also an interesting model, as the bone is an organ extensively exposed to AgNPs due to its use in bone and dental implants, medical devices and bone cement [84].

The CBMN cyt assay conditions used in A549 cell line, 4.5 µg/mL of cyt-B, with a time of exposure of 29h, were replicated in MG-63 cell line, along with 3 µg/mL of cyt-B (the minimum of the usually range of 3 to 6 µg/mL [64]) with a time of exposure of 35h. For 4.5 µg/mL of cyt-B, in both times, although the cells were binucleated, the number of necrotic and apoptotic cells was too high (approximately 50%). When 3 µg/mL of cyt-B was used the cells were healthy. Considering the duration of the exposure, when the time of exposure was 29h, the amount of binucleated cells was still low (around 30%), but for 35h of exposure, almost all cells were binucleated (Table 6). Altogether, it was realized that the conditions 3 µg/mL of cyt-B with a time of exposure of 35h were the most suitable.

Table 6 : Qualitative study with the aim of optimization of the parameters "Concentration of cytochalasin-B" and "time of exposure" for MG-63 cell line. The X represents the non-viable state of cells; the ✓∓ represents the existence of healthy cells, however with a low percentage of binucleated ones; the ✓ represents de existence of healthy cells, almost all binucleated

29h			35h		
[0]	[3]	[4.5]	[0]	[3]	[4.5]
✓	✓∓	X	✓	✓	X

After the optimization of the CBMN cyt assay conditions, the test was validated by exposure of MG-63 cell line to 50 and 100 µg/mL of 20 nm AgNPs.

Results showed that the number of binucleated cells was much higher than the mononucleated ones for both concentrations (Fig.11), with significant variance between them (Mononucleated cells: One way analysis, $F_{2,6}$ = 11.090, P= 0.01; Binucleated cells: One way analysis, $F_{2,6}$ = 94.184, P<0.001). For both mononucleated and binucleated cells, the control was significantly different from 50 µg/mL and 100 µg/mL.

The NDI (Fig.12) was near the ideal value of 2 for either concentrations (Kruskal-Wallis test: H = 2.756, DF=2, P= 0.296), therefore, it was considered that the CBMN assay conditions were optimized and the assay was validated for MG-63 cells line. Then the putative effects of AgNPs on DNA damage of MG-63 cells were evaluated.

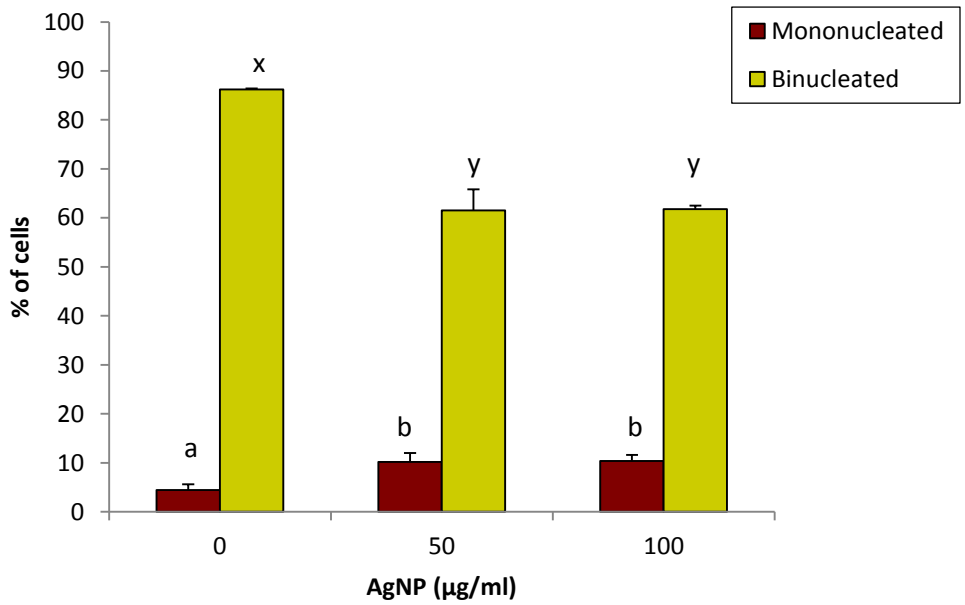

Fig. 11 Percentage of mono and binucleated cells assessed with the cytokinesis-block micronucleus cytome assay, after exposure of MG-63 cells to increasing concentrations of 20 nm AgNPs. Results are expressed as means ± standard deviation. Different letters means statistic differences between groups (p<0.05), where a and b refers to mononucleated cells, and x and y to binucleated cells.

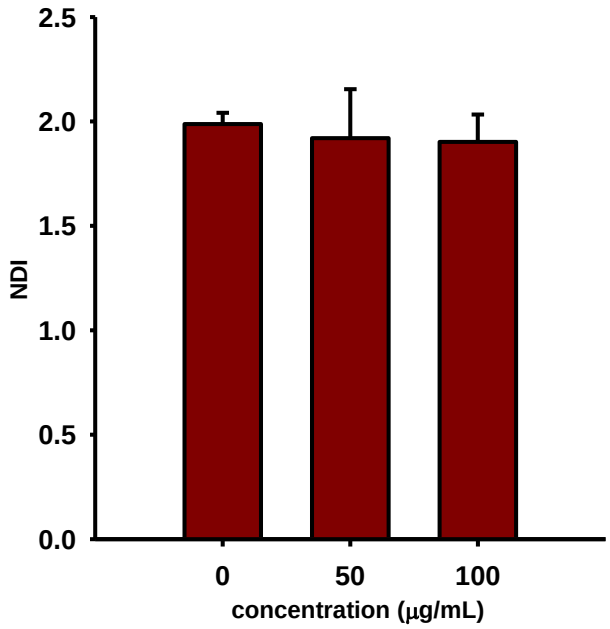

Fig. 12 Nuclear division index assessed with the cytokinesis-block micronucleus cytome assay, after exposure of MG-63 cells to 20 nm AgNPs. Results are expressed as means ± standard deviation.

A slightly increase in the number of necrotic and apoptotic cells was observed (Fig.13), in both concentrations, when compared to control. However, only necrosis, for 100 µg/mL was significant (Apoptosis: One way analysis, $F_{2,6}$= 4.261, P= 0.071; Necrosis: One way analysis, $F_{2,6}$ = 5.297, P= 0.047).

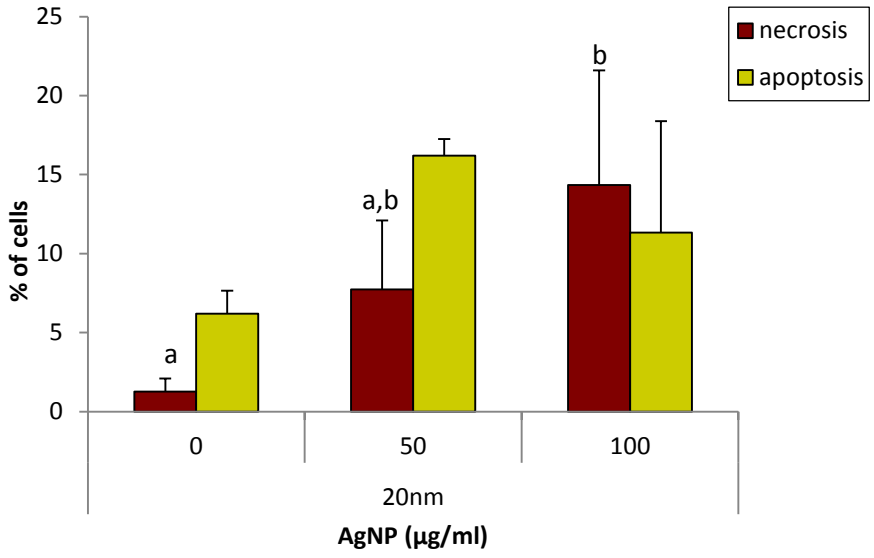

Fig. 13 Percentage of necrotic and apoptotic cells assessed with the cytokinesis-block micronucleus cytome assay, after exposure of MG-63 cells to increasing concentrations of 20 nm AgNPs. Results are expressed as means ± standard deviation. No statistical differences were found for the apoptosis. In necrosis, different letters means statistic differences between groups (p<0.05).

The parameters for the evaluation of the DNA damage, MNI, NBUDs and NPBs were then scored, and some representative images were taken (Fig.14), to better elucidate their morphologies.

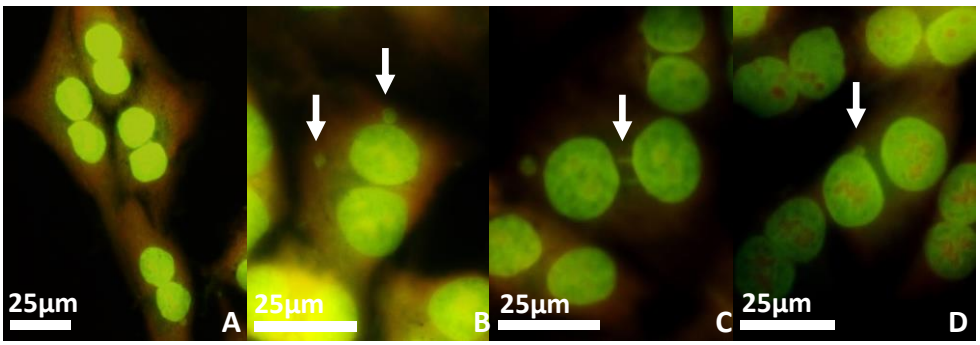

Fig. 14 Representative images obtained by fluorescence microscopy of the cytokinesis-block micronucleus cytome assay in MG-63 cells for 20 nm AgNPs: A) binucleated cells (control), B) binucelated cell with two micronuclei (50 µg/mL), C) binucleated cell with two nucleoplasmic bridges (50 µg/mL) and D) binucleated cell with one nuclear bud (50 µg/mL).

When evaluated the parameters (Fig.15), it was observed that all the three followed the same tendency, increasing for 50 µg/mL, and decreasing for 100 µg/mL. For the MNi (Kruskal-Wallis test: H = 7.200, DF=2, P=0.004) and the NBUDs (Kruskal-Wallis test: H = 7.261, DF=2, P=0.004) the increase for 50 µg/mL was significant, however, the same was not observed for the NPBs (Kruskal-Wallis test: H = 5.445, DF=2, P= 0.071). Regarding the behavior for 100 µg/mL, it may be explained by the fact that when the concentration of AgNPs increase, the behavior of aggregation would also increase [73]. A consequence of that aggregation behavior would be the reducing of the surface area of AgNPs, to which the cells may be exposed, probably decreasing their toxicity. However, in a previous study by Rosário (Rosário, 2012, Effects of silver nanoparticles on osteosarcoma and lung cell lines, UA, Aveiro, Portugal), was found that 20 nm AgNPs diluted in α-MEM (the medium in which MG-63 cells were cultured) had a less tendency to aggregate, comparing to the ones diluted in F-12K, justifying the need of a careful characterization, and suggesting other ways of action of the AgNPs.

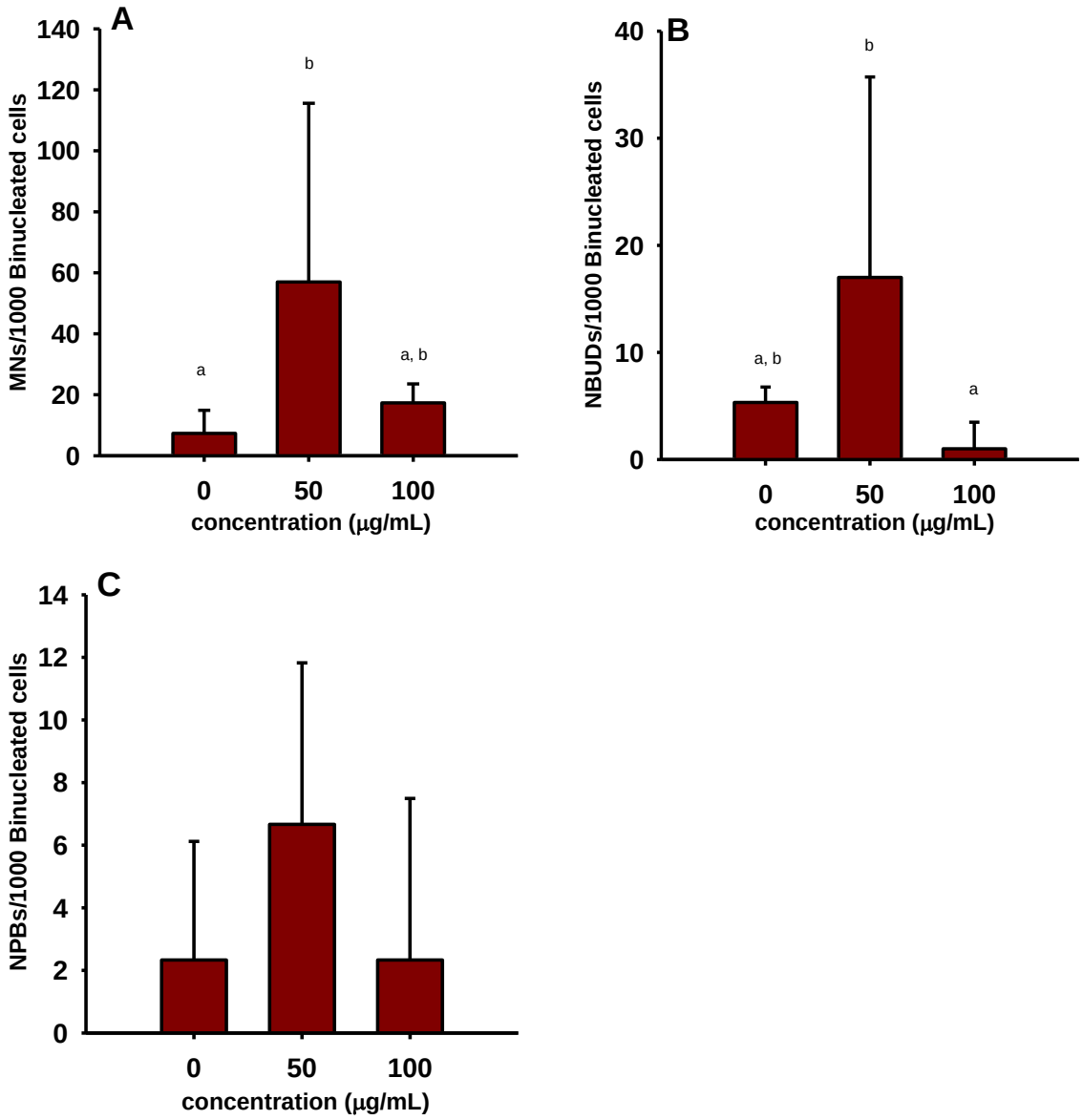

Fig. 15 Assessed parameters with the cytokinesis-block micronucleus cytome assay to evaluate DNA damage, after exposure of MG-63 cells to 20 nm AgNPs: A) Micronucleus (MNi) per 1000 binucleated cells; B) Nuclear buds (NBUDs) per 1000 binucleated cells and C) Nucleoplasmic bridges (NPBs) per 1000 binucleated cells. Results are expressed as means ± standard deviation. Different letters means statistic differences between groups ($p<0.05$).

The presence of MNi, NBUDs and NPBs in the CBMN cyt assay may be indicative of a large number of disturbances, affecting both the chromosomes, the spindle fiber, the kinetochore proteins, among others [for review see 87,88]. The huge range of anomalies that can exist makes difficult to study what is really originating the disturbances.

The damage can be due to the AgNPs itself, meaning that somehow they must enter to the nucleus, by the release of Ag^{+} ions, or also by the generation of ROS both by

the AgNPs and the Ag^+ ions (Fig.16). In order to AgNPs interact directly with DNA, they must be able to diffuse into the nucleus. One possible way for that to happen is through the nuclear pore complexes [38]. The pores have an effective diameter of 9-10 nm, so, 10 nm AgNPs, if not aggregated, may be able to diffuse inside the nucleus, but not 20 nm AgNPs, at least by this way.

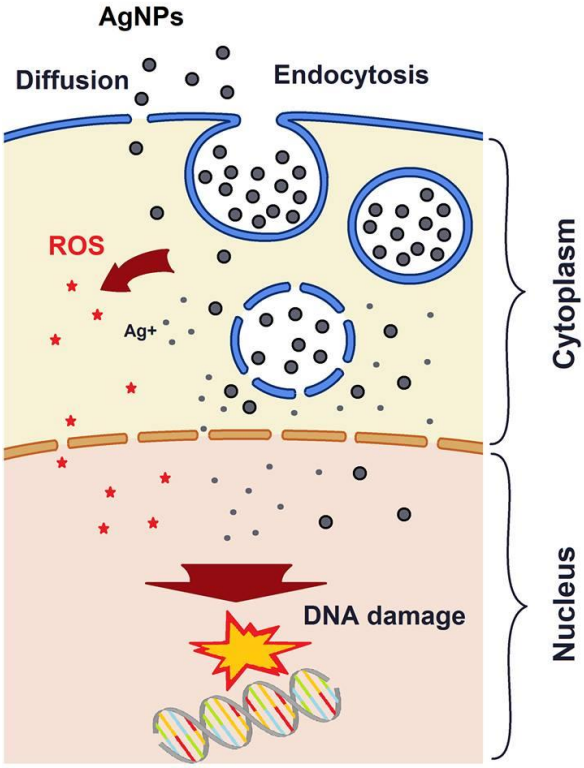

Fig. 16 Proposed forms of AgNPs interaction with DNA: i) direct interaction of the AgNP; ii) interaction of the Ag^+ dissolved ion; iii) indirectly by the formed ROS.

Previous reports [34] described 20 nm AgNPs inside the nucleus of A549 cells, meaning that may exist another possible route of entry. However, another report by Greulich *et al.* [87] described that 80 nm PVP-AgNPs were able to enter into hMSC cells, but not into their nuclei. Altogether, these results show that there are different ways of entrance of AgNPs into the nucleus, however they should be also size-dependent. Once inside the nucleus, AgNPs may interact directly with the DNA. In fact, a preliminary report by Basu *et al.* [88] showed the possible interaction of AgNPs with DNA bases, showing the preference of the interactions: C>G>A>T. However, the lack of genotoxic studies does not allow yet to infer how the AgNPs interact *in vitro* and *in vivo* with the DNA itself. The interaction can also happen by the release of Ag^+ ions from AgNPs. Although it is not

consensual, the evidences suggest that Ag^+ ion account in some part for the AgNP toxicity [50]. Once inside the cell, the AgNPs may release Ag^+ ions, with the size of the nanoparticles influencing the kinetics of dissolution. The smallest nanoparticles dissolved faster and to a larger extent [89], and posteriorly may induce the production of ROS that consequently lead to oxidative stress [38]. The Ag^+ ions can also diffuse inside the nucleus and interact directly with proteins containing –thiol groups [90]. The easier diffusion of smaller nanoparticles inside the nucleus, along with the larger extent of smaller nanoparticles, may explain the lower DNA damage with the 20 nm AgNPs in the comet assay.

4. Conclusions and Future Perspectives

4. Conclusions and future perspectives

The present work showed the genotoxic potential of PVP coated AgNPs in two different cell lines, of lung and bone. In A549 cell line both sizes of AgNPs (10 and 20 nm), were able to induce DNA damage, with the smaller being more toxic. Also, a cytostatic effect induced by the AgNPs was observed.

To our knowledge, this is the first study that shows DNA damage induced by AgNPs in bone cells. In MG-63 cell line the 20nm AgNPS induced both MNi and NBUDs in the lower concentration, indicating the presence of DNA damage.

In future work, in order to complement the observations made with the comet assay for A549 cell line, and with the cytokinesis-block micronucleus cytome assay in MG-63 cell line, the missing assays should be performed, along with the FPG-modified comet assay. The quantification of dissolved Ag^+ ions would be also important, together with the individual study of the effects made by AgNPs and by the Ag^+ ions, to better understand which one more contributes to the toxicity.

5. Bibliography

5. Bibliography

1. Singh M, S.Manikandan, A.K.Kumaraguru. 2010. Nanopaticles: A New Technology with Wide Applications. *Res. J. Nanosci. Nanotechnol.* doi:10.3923/rjnn.2010.
2. Faraday M. 1857. Experimental Relations of Gold (and Other Metals) to Light. *Philos. Trans. R. Soc. London*. 147:145–181.
3. Kreuter J. 2007. Nanoparticles—a historical perspective. *Int. J. Pharm.* 331:1–10.
4. Love S, Maurer-Jones M, Thompson J, Lin Y-S, Haynes C. 2012. Assessing nanoparticle toxicity. *Annu. Rev. Anal. Chem.* 5:181–205.
5. Lai DY. 2012. Toward toxicity testing of nanomaterials in the 21st century: a paradigm for moving forward. *WIREs Nanomed and nanobiotechnol*. 4:1–15.
6. Buzea C, Pacheco II, Robbie K. 2007. Nanomaterials and nanoparticles: Sources and toxicity. *Biointerphases*. 2:MR17.
7. Lidén G. 2011. The European commission tries to define nanomaterials. *Ann. Occup. Hyg.* 55:1–5.
8. Farré M, Sanchís J, Barceló D. 2011. Analysis and assessment of the occurrence, the fate and the behavior of nanomaterials in the environment. *Trends Anal. Chem.* 30:517–527.
9. Nowack B, Bucheli TD. 2007. Occurrence, behavior and effects of nanoparticles in the environment. *Environ. Pollut.* 150:5–22.
10. EMPA. 2012. *Nanomaterials in waste incineration and landfills*.:1–70.
11. Li Q, Hub X, Bai Y, Alattar M, Maa D, Cao Y, Hao Y, Wang L, Jiang C. 2013. The oxidative damage and inflammatory response induced by lead. *Food Chem. Toxicol.* 60:213–7.
12. Liu M, Gu X, Zhang K, Ding Y, Wei X, Zhang X, Zhao Y. 2013. Gold nanoparticles trigger apoptosis and necrosis in lung cancer cells with low intracellular glutathione. *J. Nanoparticle Res.* 15:1745.
13. Alarifi S, Ali D, Verma A, Alakhtani S, Ali BA. 2013. Cytotoxicity and genotoxicity of copper oxide nanoparticles in human skin keratinocytes cells. *Int. J. Toxicol.* 32:296–307.
14. Alarifi S, Ali D, Alkahtani S, Verma A, Ahamed M, Ahmed M, Alhadlaq H a. 2013. Induction of oxidative stress, DNA damage, and apoptosis in a malignant human skin melanoma cell line after exposure to zinc oxide nanoparticles. *Int. J. Nanomedicine*. 8:983–93.
15. Ahamed M, Alhadlaq HA, Javed Alam MAMK, Ali D, Alarafi S. 2013. Iron Oxide Nanoparticle-induced Oxidative Stress and Genotoxicity in Human Skin Epithelial and Lung Epithelial Cell Lines. *Curr. Pharm. Des.* 19:6681–6690.
16. Kim S, Ryu D-Y. 2013. Silver nanoparticle-induced oxidative stress, genotoxicity and apoptosis in cultured cells and animal tissues. *J. Appl. Toxicol.* 33:78–89.
17. Dibrov P, Dzioba J, Gosink KK, Ha CC. 2002. Chemiosmotic Mechanism of Antimicrobial Activity of Ag+ in Vibrio cholerae. *Antimicrob. Agents Chemother.* 46:2668–2670.
18. Benn TM, Westerhoff P. 2008. Nanoparticle silver released into water from commercially available sock fabrics. *Environ. Sci. Technol.* 42:4133–9.

19. You C, Han C, Wang X, Zheng Y, Li Q, Hu X, Sun H. 2012. The progress of silver nanoparticles in the antibacterial mechanism, clinical application and cytotoxicity. *Mol. Biol. Rep.* 39:9193–201.
20. Chen X, Schluesener HJ. 2008. Nanosilver: a nanoproduct in medical application. *Toxicol. Lett.* 176:1–12.
21. Sur I, Altunbek M, Kahraman M, Culha M. 2012. The influence of the surface chemistry of silver nanoparticles on cell death. *Nanotechnology*. 23:375102.
22. Singh RP, Ramarao P. 2012. Cellular uptake, intracellular trafficking and cytotoxicity of silver nanoparticles.pdf. *Toxicol. Lett.* 213:249–259.
23. Tolaymat TM, El Badawy AM, Genaidy A, Scheckel KG, Luxton TP, Suidan M. 2010. An evidence-based environmental perspective of manufactured silver nanoparticle in syntheses and applications: a systematic review and critical appraisal of peer-reviewed scientific papers. *Sci. Total Environ.* 408:999–1006.
24. Kim JS, Sung JH, Ji JH, Song KS, Lee JH, Kang CS, Yu IJ. 2011. In vivo Genotoxicity of Silver Nanoparticles after 90-day Silver Nanoparticle Inhalation Exposure. *Saf. Health Work*. 2:34–8.
25. Chaudhry Q, Scotter M, Blackburn J, Ross B, Boxall A, Castle L, Aitken R, Watkins R. 2008. Applications and implications of nanotechnologies for the food sector. *Food Addit. Contam.* 25:241–58.
26. Ju-Nam Y, Lead JR. 2008. Manufactured nanoparticles: an overview of their chemistry, interactions and potential environmental implications. *Sci. Total Environ.* 400:396–414.
27. Ahamed M, Alsalhi MS, Siddiqui MKJ. 2010. Silver nanoparticle applications and human health. *Int. J. Clin. Chem.* 411:1841–8.
28. Lara HH, Ayala-Nuñez N V, Ixtepan-Turrent L, Rodriguez-Padilla C. 2010. Mode of antiviral action of silver nanoparticles against HIV-1. *J. Nanobiotechnology*. 8:1.
29. Galdiero S, Falanga A, Vitiello M, Cantisani M, Marra V, Galdiero M. 2011. Silver nanoparticles as potential antiviral agents. *Molecules*. 16:8894–918.
30. Baram-Pinto D, Shukla S, Perkas N, Gedanken A, Sarid R. 2009. Inhibition of herpes simplex virus type 1 infection by silver nanoparticles capped with mercaptoethane sulfonate. *Bioconjug. Chem.* 20:1497–502.
31. Rogers J V., Parkinson C V., Choi YW, Speshock JL, Hussain SM. 2008. A Preliminary Assessment of Silver Nanoparticle Inhibition of Monkeypox Virus Plaque Formation. *Nanoscale Res. Lett.* 3:129–133.
32. Mailänder V, Landfester K. 2009. Interaction of Nanoparticles with Cells. *Biomacromolecules*. 10:2379–2400.
33. Bartłomiejczyk T, Lankoff A, Kruszewski M, Szumiel I. 2013. Silver nanoparticles -- allies or adversaries? *Ann. Agric. Environ. Med.* 20:48–54.
34. Kruszewski M, Brzoska K, Brunborg G, Asare N. 2011. Toxicity of silver nanomaterials in higher eukaryotes. *Adv. Mol. Toxicol.* 5:179–218.
35. Arora S, Jain J, Rajwade JM, Paknikar KM. 2008. Cellular responses induced by silver nanoparticles: In vitro studies. *Toxicol. Lett.* 179:93–100.
36. Hussain SM, Hess KL, Gearhart JM, Geiss KT, Schlager JJ. 2005. In vitro toxicity of nanoparticles in BRL 3A rat liver cells. *Toxicol. Vitr.* 19:975–83.

37. Carlson C, Hussain SM, Schrand a M, Braydich-Stolle LK, Hess KL, Jones RL, Schlager JJ. 2008. Unique cellular interaction of silver nanoparticles: size-dependent generation of reactive oxygen species. *J. Phys. Chem. B*. 112:13608–19.
38. AshaRani P V, Low Kah Mun G, Hande MP, Valiyaveettil S. 2009. Cytotoxicity and genotoxicity of silver nanoparticles in human cells. *ACS Nano*. 3:279–90.
39. Ghosh M, J M, Sinha S, Chakraborty A, Mallick SK, Bandyopadhyay M, Mukherjee A. 2012. In vitro and in vivo genotoxicity of silver nanoparticles. *Mutat. Res.* 749:60–9.
40. Lankoff A, Sandberg WJ, Wegierek-Ciuk A, Lisowska H, Refsnes M, Sartowska B, Schwarze PE, Meczynska-Wielgosz S, Wojewodzka M, Kruszewski M. 2012. The effect of agglomeration state of silver and titanium dioxide nanoparticles on cellular response of HepG2, A549 and THP-1 cells. *Toxicol. Lett.* 208:197–213.
41. Bouwmeester H, Poortman J, Peters RJ, Wijma E, Kramer E, Makama S, Puspitaninganindita K, Marvin HJP, Peijnenburg AACM, Hendriksen PJM. 2011. Characterization of translocation of silver nanoparticles and effects on whole-genome gene expression using an in vitro intestinal epithelium coculture model. *ACS Nano*. 5:4091–103.
42. Böhmert L, Niemann B, Thünemann AF, Lampen A. 2012. Cytotoxicity of peptide-coated silver nanoparticles on the human intestinal cell line Caco-2. *Arch. Toxicol.* 86:1107–15.
43. Orlowski P, Krzyzowska M, Zdanowski R, Winnicka A, Nowakowska J, Stankiewicz W, Tomaszewska E, Celichowski G, Grobelny J. 2013. Assessment of in vitro cellular responses of monocytes and keratinocytes to tannic acid modified silver nanoparticles. *Toxicol. Vitr.* 27:1798–1808.
44. Kang K, Jung H, Lim J-S. 2012. Cell Death by Polyvinylpyrrolidine-Coated Silver Nanoparticles is Mediated by ROS-Dependent Signaling. *Biomol. Ther. (Seoul).* 20:399–405.
45. Lin J-J, Lin W-C, Dong R-X, Hsu S. 2012. The cellular responses and antibacterial activities of silver nanoparticles stabilized by different polymers. *Nanotechnology*. 23:065102.
46. Kaur J, Tikoo K. 2013. Evaluating cell specific cytotoxicity of differentially charged silver nanoparticles. *Food Chem. Toxicol.* 51:1–14.
47. Song X, Li B, Xu K, Liu J, Ju W, Wang J, Liu X, Li J, Qi Y. 2012. Cytotoxicity of water-soluble mPEG-SH-coated silver nanoparticles in HL-7702 cells. *Cell Biol. Toxicol.* 28:225–37.
48. Chairuangkitti P, Lawanprasert S, Roytrakul S, Aueviriyavit S, Phummiratch D, Kulthong K, Chanvorachote P, Maniratanachote R. 2013. Silver nanoparticles induce toxicity in A549 cells via ROS-dependent and ROS-independent pathways. *Toxicol. Vitr.* 27:330–8.
49. Suliman AO, Ali D, Alarifi S, Harrath AH, Mansour L. 2013. Evaluation of Cytotoxic , Oxidative stress , Proinflammatory and Genotoxic Effect of Silver Nanoparticles in Human Lung Epithelial Cells. *Wiley Period.*1–12. doi:10.1002/tox.
50. Beer C, Foldbjerg R, Hayashi Y, Sutherland DS, Autrup H. 2012. Toxicity of silver nanoparticles—Nanoparticle or silver ion? *Toxicol. Lett.* 208:286–292.

51. Kim S, Choi JE, Choi J, Chung K-H, Park K, Yi J, Ryu D-Y. 2009. Oxidative stress-dependent toxicity of silver nanoparticles in human hepatoma cells. *Toxicol. Vitr.* 23:1076–1084.
52. McKenna DJ, McKeown SR, McKelvey-Martin VJ. 2008. Potential use of the comet assay in the clinical management of cancer. *Mutagenesis*. 23:183–90.
53. Franco R, Sánchez-Olea R, Reyes-Reyes EM, Panayiotidis MI. 2009. Environmental toxicity, oxidative stress and apoptosis: ménage à trois. *Mutat. Res.* 674:3–22.
54. Kim HR, Park YJ, Shin DY, Oh SM, Chung KH. 2013. Appropriate in vitro methods for genotoxicity testing of silver nanoparticles. *Environ. Health Toxicol.* 28:e2013003.
55. Ostling O, Johanson KJ. 1984. Microelectrophoretic study of radiation-induced DNA damages in individual mammalian cells. *Biochem. Biophys. Res. Commun.* 123:291–298.
56. Singh NP, McCoy MT, Tice RR, Schneider EL. 1988. A simple technique for quantitation of low levels of DNA damage in individual cells. *Exp. Cell Res.* 175:184–191.
57. Kumaravel TS, Vilhar B, Faux SP, Jha AN. 2009. Comet Assay measurements: a perspective. *Cell Biol. Toxicol.* 25:53–64.
58. Olive PL, Durand RE. 1992. Detection of hypoxic cells in a murine tumor with the use of the comet assay. *J. Natl. Cancer Inst.* 84:707–11.
59. Hartmann A, Agurell E, Beevers C, Smith A, Speit G, Thybaud V, Tice RR. 2003. Recommendations for conducting the in vivo alkaline Comet assay. *Mutagenesis*. 18:45–51.
60. Collins A, Dušinská M, Franklin M, Somorovská M, Petrovská H, Susan Duthie. 1997. Comet Assay in Human Biomonitoring Studies : Reliability , Validation , and Applications. *Environ. Mol. Mutagen.* 30:139–146.
61. Jha AN. 2004. Genotoxicological studies in aquatic organisms: an overview. *Mutat. Res.* 552:1–17.
62. Gaivão I, Piasek A, Brevik A, Shaposhnikov S, Collins AR. 2009. Comet assay-based methods for measuring DNA repair in vitro; estimates of inter- and intra-individual variation. *Cell Biol. Toxicol.* 25:45–52.
63. Gonzalez L, Sanderson BJS, Kirsch-Volders M. 2011. Adaptations of the in vitro MN assay for the genotoxicity assessment of nanomaterials. *Mutagenesis*. 26:185–91.
64. OECD. 2006. *OECD GUIDELINE FOR THE TESTING OF CHEMICALS DRAFT PROPOSAL FOR A NEW GUIDELINE 487 : In Vitro Micronucleus Test*.:1–16.
65. Fenech M. 2007. Cytokinesis-block micronucleus cytome assay. *Nat. Protoc.* 2:1084–104.
66. Fenech M. 2000. The in vitro micronucleus technique. *Mutat. Res.* 455:81–95.
67. Oberdörster G, Sharp Z, Atudorei V, Elder a, Gelein R, Kreyling W, Cox C. 2004. Translocation of inhaled ultrafine particles to the brain. *Inhal. Toxicol.* 16:437–45.
68. Foster K a, Oster CG, Mayer MM, Avery ML, Audus KL. 1998. Characterization of the A549 cell line as a type II pulmonary epithelial cell model for drug metabolism. *Exp. Cell Res.* 243:359–366.
69. Jaramillo ML, Banville M, Collins C, Paul-Roc B, Bourget L, O'Connor-McCourt M. 2008. Differential sensitivity of A549 non-small lung carcinoma cell responses to epidermal growth factor receptor pathway inhibitors. *Cancer Biol. Ther.* 7:557–568.

70. Tice RR, Agurell E, Anderson D, Burlinson B, Hartmann a, Kobayashi H, Miyamae Y, Rojas E, Ryu JC, Sasaki YF. 2000. Single cell gel/comet assay: guidelines for in vitro and in vivo genetic toxicology testing. *Environ. Mol. Mutagen.* 35:206–21.
71. Lee YS, Kim DW, Lee YH, Oh JH, Yoon S, Choi MS, Lee SK, Kim JW, Lee K, Song C-W. 2011. Silver nanoparticles induce apoptosis and G2/M arrest via PKCzeta-dependent signaling in A549 lung cells. *Arch. Toxicol.* 85:1529–40.
72. Mwilu SK, El Badawy AM, Bradham K, Nelson C, Thomas D, Scheckel KG, Tolaymat T, Ma L, Rogers KR. 2013. Changes in silver nanoparticles exposed to human synthetic stomach fluid: effects of particle size and surface chemistry. *Sci. Total Environ.* 447:90–98.
73. El Badawy AM, Scheckel KG, Suidan M, Tolaymat T. 2012. The impact of stabilization mechanism on the aggregation kinetics of silver nanoparticles. *Sci. Total Environ.* 429:325–31.
74. De Marzi L, Monaco A, De Lapuente J, Ramos D, Borras M, Di Gioacchino M, Santucci S, Poma A. 2013. Cytotoxicity and genotoxicity of ceria nanoparticles on different cell lines in vitro. *Int. J. Mol. Sci.* 14:3065–77.
75. Bhattacharya K, Naha PC, Naydenova I, Mintova S, Byrne HJ. 2012. Reactive oxygen species mediated DNA damage in human lung alveolar epithelial (A549) cells from exposure to non-cytotoxic MFI-type zeolite nanoparticles. *Toxicol. Lett.* 215:151–60.
76. Liu W, Wu Y, Wang C, Li HC, Wang T, Liao CY, Cui L, Zhou QF, Yan B, Jiang GB. 2010. Impact of silver nanoparticles on human cells: effect of particle size. *Nanotoxicology*. 4:319–30.
77. Kruszewski M, Grądzka I, Bartłomiejczyk T, Chwastowska J, Sommer S, Grzelak A, Zuberek M, Lankoff A, Dusinska M, Wojewódzka M. 2013. Oxidative DNA damage corresponds to the long term survival of human cells treated with silver nanoparticles. *Toxicol. Lett.* 219:151–159.
78. Yang H, Liu C, Yang D, Zhang H, Xi Z. 2009. Comparative study of cytotoxicity, oxidative stress and genotoxicity induced by four typical nanomaterials: the role of particle size, shape and composition. *J. Appl. Toxicol.* 29:69–78.
79. Azqueta A, Collins AR. 2013. The essential comet assay: a comprehensive guide to measuring DNA damage and repair. *Arch. Toxicol.* 87:949–68.
80. Asharani P V, Hande MP, Valiyaveettil S. 2009. Anti-proliferative activity of silver nanoparticles. *BMC Cell Biol.* 10:65.
81. Kang SJ, Lee YJ, Lee E-K, Kwak M-K. 2012. Silver nanoparticles-mediated G2/M cycle arrest of renal epithelial cells is associated with NRF2-GSH signaling. *Toxicol. Lett.* 211:334–41.
82. Lee YS, Yoon H-J, Oh J-H, Park H-J, Lee E-H, Song C-W, Yoon S. 2009. 1,3-Dinitrobenzene induces apoptosis in TM4 mouse Sertoli cells: Involvement of the c-Jun N-terminal kinase (JNK) MAPK pathway. *Toxicol. Lett.* 189:145–51.
83. Zhang L, Zhang J, Hu C, Cao J, Zhou X, Hu Y. 2009. Efficient activation of p53 pathway in A549 cells exposed to L2, a novel compound targeting p53–MDM2 interaction. *Anticancer. Drugs*. 20:416–424.
84. Zheng Y, Li J, Liu X, Sun J. 2012. Antimicrobial and osteogenic effect of Ag-implanted titanium with a nanostructured surface. *Int. J. Nanomedicine*. 7:875–84.

85. Kumar A, Dhawan A. 2013. Genotoxic and carcinogenic potential of engineered nanoparticles: an update. *Arch. Toxicol.* 87:1883–900.
86. Fenech M, Kirsch-Volders M, Natarajan AT, Surralles J, Crott JW, Parry J, Norppa H, Eastmond D a, Tucker JD, Thomas P. 2011. Molecular mechanisms of micronucleus, nucleoplasmic bridge and nuclear bud formation in mammalian and human cells. *Mutagenesis*. 26:125–32.
87. Greulich C, Diendorf J, Simon T, Eggeler G, Epple M, Köller M. 2011. Uptake and intracellular distribution of silver nanoparticles in human mesenchymal stem cells. *Acta Biomater.* 7:347–54.
88. Basu S, Jana S, Pande S, Pal T. 2008. Interaction of DNA bases with silver nanoparticles: assembly quantified through SPRS and SERS. *J. Colloid Interface Sci.* 321:288–93.
89. Liu J, Sonshine DA, Shervani S, Hurt RH. 2010. Controlled release of biologically active silver from nanosilver surfaces. *ACS Nano*. 4:6903–13.
90. Behra R, Sigg L, Clift MJD, Herzog F, Minghetti M, Johnston B, Rothen-rutishauser B, Petri-fink A. 2013. Chemical and biochemical perspective Bioavailability of silver nanoparticles and ions : from a chemical and biochemical perspective. *J. R. Soc.* 10.